Theory of FRACTIONAL QUANTUM HALL EFFECT

A PROJECT PRESENTED

BY

ENDALEKACHEW HUNDE BIRU

SUBMITTED

TO

THE DEPARTMENT 0F PHYSICS

IN PARTIAL FULFILLMENT OF THE

REQUIREMENTS FOR THE DEGREE OF

MASTER OF SCIENCE IN PHYSICS

ADDIS ABABA UNIVERSITY

ADDIS ABABA, ETHIOPIA

April 2012

ADDIS ABABA UNIVERSITY

School of Graduate Studies

Department of Physics

Author: **ENDALEKACHEW HUNDE BIRU**

Title: **Theory of FRACTIONAL QUANTUM HALL EFFECT**

Approved by

Advisor: _____

Dr. Tesgera Bedassa

Examiner: _____

Prof. Vadim N. Maln'ev

Chairman: _____

Dr. Lemi Demeyu

Table of Contents

List of Figures

Abstract

This project is devoted to the investigation of the modern state of the problem connected with quantum Hall effect (integral and fractional). The quantum Hall effect is a quantum-mechanical version of the Hall effect, observed in two dimensional electron systems subjected to low temperatures ($< 1K$) and strong magnetic fields ($\sim 10T$), in which the Hall conductance$\sigma(\boldsymbol{B})$ takes on the quantized values($\frac{\nu e^2}{h}$) with ν an integer (integer quantized Hall effect) or a rational fraction (fractional quantized Hall effect), independent of the detail of the sample geometry. in this project we see detail description of fractional quantum hall effect by using some theories, It starts from the LAUGHLIN states and their generalization following JAIN's picture of composite fermions. The work of this project ends with a description of the fractional quantum hall effect in graphene, since graphene is two dimensional carbon and carbon atoms in graphene, shows electron-electron interaction thus we must expect fractional quantum hall effect in graphene

Acknowledgements

Above all, I would like to thank the almighty; God, for letting me to accomplish this stage.

In any case, there are a lot of people of which I'm grateful for supporting me during this period. First of all I would like to give my thanks to my adviser, Dr. Tesgera Bedassa. Not only for providing me with a project subject of which I wasn't even aware it existed, but also for keeping his door open for questions, even the trivial ones, keeping the material comprehensible and providing me with the proper guidance.

Secondly, I am indebted to all the teachers of the Department of Physics at the Addis Ababa University for the academic culture and the knowledge they granted me.

Thirdly, I want to acknowledge the ministry of education for providing the scholarship that has funded my master studies in physics.

Last but not least, my strongest thank is addressed to my Families, who lived for myself. They are the hero of my success without their push and support, this stage is unthinkable.

Introduction

In this project, mainly I try to provide description of fractional quantum Hall effect by using some theories like: laughlin's trial wave function, Plasma Analogy, Fractionally Charged Excitations, Composite-fermion approach and Hierarchies. At the end of the project, I will try to see fractional quantum Hall effect in graphene.

In the last decades the impressive development of semiconductor devices has made possible to realize systems where the quantum properties clearly appear also at the macroscopic level showing their paradoxical and unconventional nature. In fact, nowadays, it is possible to create electron systems at reduced dimensionality where the correlation effects become dominant. These kinds of systems have attracted attention both from the experimental and the theoretical point of view. Probably one of the most important examples is the quantum Hall effect that even today, thirty years after its discovery, remains a fundamental topic in the agenda of the condensed matter physics. This effect appears in a two dimensional electron gas, created at the interface of two semiconductors, under a strong magnetic field and at low temperature. The Hall resistance deviates from the classical behavior showing a peculiar plateau structure. This quantization is precise to one part in 10^8 and has become the standard of resistance. In correspondence of these plateaux the longitudinal resistance drops to zero with an intriguing analogy with other systems showing a macroscopic quantum phase, namely the superconductors. The first experimental evidence of this phenomenology is due to K. von Klitzing that, in 1980, observed the quantization of the Hall resistance at integer values. This discovery motivated the Nobel Prize in physics he won in 1985. This phenomenon, known as the integer quantum Hall effect, found a convincing explanation in term of the quantum mechanical description of non interacting electrons under magnetic field, i.e. in terms of Landau levels. The so called filling factor ν represents the number of occupied levels and, in the integer quantum Hall effect, it assumes integer values.

Shortly after, in 1982, a quantization for fractional values of the filling factor has been observed by D. C. Tsui and H. L. Stormer. Despite the fact that the phenomenology involved in the fractional regime is analogous to the one in the integer, its physical interpretation requires the introduction of a new paradigm for the description of strongly interacting systems and the emergent phenomena associated with them. Indeed, in this case, the correlation between electrons cannot be neglected and the problem becomes intrinsically many-body. The following years R. Laughlin provided the first explanation in terms of a variational wavefunction. The fractional quantum Hall effect (FQHE) at the Landau-level (LL) filling fraction $\nu = 1/m$ with m an old integer is very well described by Laughlin's theory. Laughlin together with the experimentalists that discovered the effect, he received the Nobel Prize in physics for this unconventional approach.

One of the more important consequences of Laughlin's idea is the prediction of elementary excitation with fractional charge and statistics and an energy gap of creation. These excitations represent a peculiar characteristic of the fractional quantum Hall effect. An important generalization of the Laughlin's work, able to explain a larger class of states in the fractional regime, is due to J. K. Jain that introduced the idea of composite fermions.

The Laughlin wave function is a very good approximation of the exact ground state of the quantum Hall effect (QHE) at $\nu = \frac{1}{m}$. However for the FQHE at $\neq \frac{1}{m}$, there exist two well-known theories. One is the hierarchical theory proposed by Haldane and Halperin. The states at $\nu = \frac{1}{m}$ are formed due to the condensation of the anyonic quasiparticles of Laughlin states. The trial wave functions constructed from this theory are called as the hierarchical wave functions.

Another theory is based on the composite fermion (CF) approach proposed by Jain, where the FQHE is due to the integer QHE of the composite fermions (CFs) (electrons bounded with an even magnetic flux quanta). The trial wave functions constructed from the CF theory are called the CF wave functions (or Jain's wave functions). The overlaps of the exact states with the hierarchical wave functions and the CF wave functions are both excellent. It has also been shown that two theories predict the same topological excitations at the same ν. The two theories must be physically equivalent if they both describe correctly the physics of the FQHE.

Graphene is the recently discovered two-Dimension allotropic from of carbon. In graphene, the structure of the honeycomb lattice endows the electron wavefunctions with an additional quantum number, termed valley isospin, which, combined with the usual electron spin, yields four-fold degenerate Landau levels (LLs). This additional symmetry modifies the QHFM and FQHE with intriguing interplay between two different spin flavours. As a consequence, it is conjectured to produce new incompressible ground states in graphene, reflecting strong electron interactions. In this presentation we report multiterminal measurements of the FQHE in high mobility graphene devices fabricated on hexagonal boron nitride substrates.

In this project we will discuss fractional quantum hall effect and some theories of fractional quantum hall effect.

This project is divided into five Chapters:

In **Chapter 1** we will briefly discuss classical hall effect and magneto- transport in the crystal due to the simultaneous presence of electric and magnetic fields with one or two types of charge carrier in the crystal.

In **Chapter 2** we will discuss a two dimensional electron gas and how it is possible to create a two dimensional electron gas and also will see landau level

In **Chapter 3** we introduction the quantum Hall effect. The goal is an intuitive understanding of the effect and the formation of plateaux and we see how it can to be related to classical effect.

In **Chapter 4** we discuss the integer quantum hall effect. Under this topic we will try to show quantization of conductivity in quantum hall effect, by using two arguments, namely: Laughlin's Gendanken-Experiment and B$\ddot{u}$ttiker's Theory of Edge Currents

In **Chapter 5** this chapter is a fairly large introduction into the fractional quantum Hall effect and some theories of fractional quantum hall effect starting from Laughlin trial wave function approach and end with Hierarchical.

Finally under this chapter we will discuss fractional quantum hall effect in graphene. Since graphene is perfect two-dimension of carbon atom and due to coulomb interaction between electron in single carbon layer we expect theoretical, fractional quantum hall effect in graphene.

CHAPTER ONE

CLASSICAL HALL EFFECT

Edward H. Hall discovered what is now known as the Hall effect in 1880. In essence, Hall's experiment consisted of a magnetic field applied perpendicular to thin plate of metal through which current was passed ($see\ Fig.1$)[1].

The current carrying particles in the metal are subjected to a Lorentz force

$$\boldsymbol{F} = e\boldsymbol{v}\ x\ \boldsymbol{B}. \tag{1.1}$$

where e is the electronic charge, $\boldsymbol{v}$ is the charge velocity and $\boldsymbol{B}$ is the magnetic field strength. The force $\boldsymbol{F}$ in the plane of motion of the charge carrier and so an electric field $\boldsymbol{E}$ is set up in the plane of the conductor perpendicular to the other vector involved.

As a direct consequence of this Lorentz force charged particle will accumulate to one side of a metal, resulting in a potential difference across the metal. In such a system one will observe an electrical potential difference between opposite points on the conductor perpendicular to the direction of the current. This voltage is the hall voltage ($\mathbf{V}_{Hall}$) and this phenomenon is called hall effect.

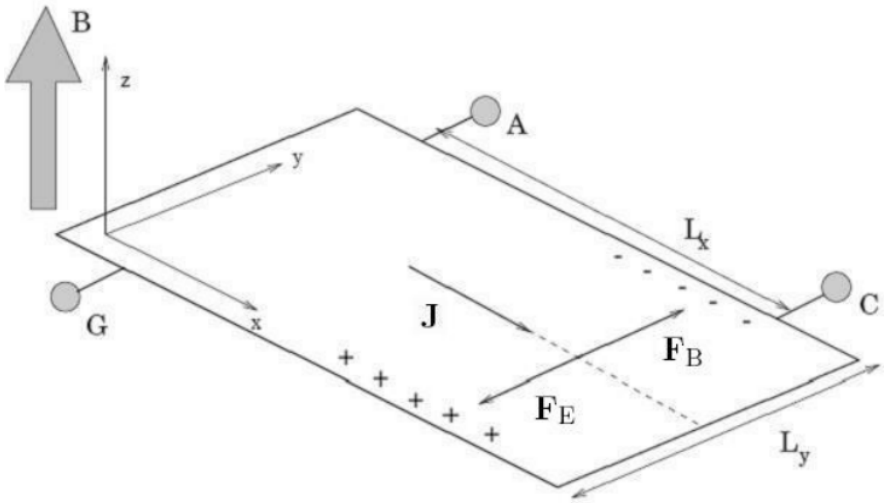

$Figure\ 1.1$: Standard geometry for Hall effect and magnetoresistivity measurements. The magnetic field **B** is along the $\hat{z}$ direction. An electric field **E** on the xy plane forces electrons to move creating a current density **J**. Due to the magnetic contribution to the Lorenz force $\mathbf{F}_B$ electrons accumulate on the upper edge of the bar. The imbalance of charge between the two edges of the sample creates an electric component of the Lorenz force $\mathbf{F}_E$. In the stationary regime, when these two components compensate, the only resulting component of the current density is along the $\hat{x}$ direction.

He considered thin metallic plates subjected to a perpendicular magnetic field $\boldsymbol{B} = \boldsymbol{B}\hat{z}$ as illustrated in $Fig.1$. After the imposition of a current along the $\hat{x}$ direction he observed a longitudinal resistance independent on the magnetic field and a transverse voltage that defines a transverse resistance, called Hall resistance, linear in $\boldsymbol{B}$ through the relation

$$\mathbf{R}_{Hall} = \frac{\boldsymbol{B}}{n_e q c}, \qquad (1.2)$$

where n_e is the electron density, c is the speed of light and q the carrier charge. By means of this relation it is possible to extract information about the nature of the carrier.

Let's consider N free electrons moving on the xy plane subjected to a perpendicular magnetic field and to an electric field on the plane. The sample dimensions are L_x along the $\hat{x}$ direction and L_y along the $\hat{y}$ direction respectively($see\ Fig.1$), with two dimensional electron density

$$n_e = \frac{N}{L_x L_y}, \qquad (1.3)$$

1.1 Magneto transport in the crystal due to the simultaneous presence of electric and magnetic fields.

In this section (under this subtopic) I want to focus on some aspects of transport phenomena due to the simultaneous presence of electric and magnetic fields; the possible presence of thermal gradients adds further variety to the phenomenology, but here we confine our attention to samples at uniform temperature.

The study of magnetic field effects on the transport properties of metals and semiconductors has become a well established and invaluable tool for the investigation of mobile carriers in crystals. In particular the Hall measurements, aimed at the determination of carrier concentration and charge sign, are routinely used for the characterization of materials. Also magnetoresistivity measurements, which determine the resistivity of materials in the presence of magnetic fields.

In isotropic media the application of an electric field drives a current density parallel and proportional to it, and the linear relationship holds(which is also known as ohm's law)[2]

$$\boldsymbol{J} = \sigma \boldsymbol{E}, \qquad (1.4)$$

where the conductivity σ is a scalar quantity. In the presence of a magnetic field, carriers are deflected and in general the current density is no more parallel to the electric field; the conductivity becomes a tensor even for an isotropic material.

The above relation (1.4) has to be replaced by the more general expression

$$\boldsymbol{J}_i = \sum_j \sigma_{ij}(\mathbf{B})\mathbf{E}_j, \quad (1.5)$$

where $\sigma_{ij}(\mathbf{B})$ $(i,j = x,y,z)$ are the components of the magnetoconductivity tensor $\sigma(\boldsymbol{B})$.

Similar considerations can be done for the resistivity of an isotropic medium in the presence of a magnetic field; the relationship between electric field and current density becomes

$$\mathbf{E}_i = \sum_j \rho_{ij}(\boldsymbol{B})\boldsymbol{J}_j, \quad (1.6)$$

where $\rho_{ij}(\boldsymbol{B})(i,j = x,y,z)$ are the components of the magnetoresistivity tensor $\rho(\boldsymbol{B})$.

The magnetoconductivity tensor and magnetoresistivity tensor are the inverse of each other, and it holds;

$$\rho_{ij}(\boldsymbol{B}) = \left(\frac{1}{\sigma(\boldsymbol{B})}\right)_{ij}, \quad (1.7)$$

The transport parameters $\rho_{ij}(\boldsymbol{B})$ are often determined experimentally using the standard geometry in which a magnetic field $\boldsymbol{B}$ is applied orthogonally to a long and thin current carrying conductor and the current flows along the x-direction $(see\ Fig.1)$.

In the standard geometry, in which transport is in the xy plane and further more $\boldsymbol{J}_y = 0$ (in stationary conditions), the current density $\boldsymbol{J}$ and the electric field $\boldsymbol{E}$ are related by[3]:

$$\begin{pmatrix}\boldsymbol{E}_x\\ \boldsymbol{E}_y\end{pmatrix} = \begin{pmatrix}\rho_{xx}(\mathbf{B}) & \rho_{xy}(\mathbf{B})\\ \rho_{yx}(\mathbf{B}) & \rho_{yy}(\mathbf{B})\end{pmatrix}\begin{pmatrix}\boldsymbol{J}_x\\ \boldsymbol{J}_y\end{pmatrix}, \quad (1.8)$$

In steady state, if the current does not flow out in y direction (i.e $\boldsymbol{J}_y = 0$).

Thus the above matrix equation can be written explicitly in the form

$$\boldsymbol{E}_x = \rho_{xx}(\mathbf{B})\boldsymbol{J}_x, \quad (1.9a)$$

$$\boldsymbol{E}_y = \rho_{yx}(\mathbf{B})\boldsymbol{J}_x, \quad (1.9b)$$

The two off-diagonal magnetoresistivity in the above matrix are given as follow

$$\rho_{yx}(\mathbf{B}) = -\rho_{xy}(\mathbf{B}), \quad (1.10)$$

The transverse electric field $\boldsymbol{E}_y$, also called Hall field, is produced by the space charges accumulated (in stationary conditions) at the borders of the conductor because of the deflection due to the magnetic field. One or the other of the off-diagonal magnetoresistivity Components $(i.e\ \rho_{yx}(\boldsymbol{B})$ or its opposite $\rho_{xy}(\boldsymbol{B})$ are also known as Hall resistivity. Most often it is convenient to report the Hall coefficient, defined as

$$R_{Hall}(\mathbf{B}) = \frac{1}{\boldsymbol{B}}\,\rho_{yx}(\mathbf{B}) = \frac{1}{\boldsymbol{B}}\frac{\boldsymbol{E}_y}{\boldsymbol{J}_x}, \qquad (1.11)$$

Notice that the Hall potential is $\mathbf{V}_{Hall} = \boldsymbol{E}_y d_y$, where d_y is the transverse dimension of the sample; in the absence of magnetic field, both $\mathbf{V}_{Hall}$ and ρ_{yx} vanish.

1.1.1 Magneto transport, when the carrier in the crystal an isotropic one-band model

I consider here Magneto transport in the case of a single type of carriers (electrons or holes) in a spherical energy band model, with unique relaxation time.

For simplicity we use a modelistic approach to the motion of electrons (or holes); the treatment with the more rigorous Boltzmann equation would give in the present case the same results. The classical equation of motion of an electron, in a dissipative medium, in the presence of an electric field $\boldsymbol{E}$ and a magnetic field $\boldsymbol{B}$ is[4]

$$m^* \frac{d\boldsymbol{v}}{dt} = (-e)\,\boldsymbol{E} + \frac{(-e)}{c}\boldsymbol{v}x\boldsymbol{B} - \frac{m^*\boldsymbol{v}}{\tau}, \qquad (1.12)$$

where m^* is the effective mass of the electron, and a damping term with constant relaxation time τ has been included.

In uniform motion conditions $\frac{d\boldsymbol{v}}{dt} = 0$, and $Eq.(1.12)$, becomes

$$\boldsymbol{v} = -e\tau\frac{\boldsymbol{E}}{m_*} - \frac{e\tau}{m_* c}\boldsymbol{v}x\mathbf{B}, \qquad (1.13)$$

We specify the above equation in the geometry of $Fig.1$, with the electric field in the xy plane and the magnetic field $\boldsymbol{B} = (0, 0, \boldsymbol{B})$ in z-direction; $Eq.(1.13)$ becomes;

$$\boldsymbol{v_x} = -\frac{e\tau}{m_*}\boldsymbol{E}_x - \omega_c\tau\boldsymbol{v_y}, \qquad (1.14a)$$

$$\boldsymbol{v_y} = -\frac{e\tau}{m_*}\boldsymbol{E}_y + \omega_c\tau\boldsymbol{v_x}, \qquad (1.14b)$$

where $\omega_c = \frac{e\boldsymbol{B}}{m^* c}$ is the cyclotron frequency. From $Eqs.(1.14a \text{ and } 1.14b)$ we have.

$$\boldsymbol{v_x} = -\frac{e\tau}{m_*}\frac{1}{1+\omega_c^2\tau^2}(\boldsymbol{E}_x - \omega_c\tau\boldsymbol{E}_y), \qquad (1.15a)$$

$$\boldsymbol{v_y} = -\frac{e\tau}{m_*}\frac{1}{1+\omega_c^2\tau^2}(\omega_c\tau\boldsymbol{E}_x + \boldsymbol{E}_y), \qquad (1.15b)$$

Thus the current density $\boldsymbol{J} = n(-e)\boldsymbol{v}$ (where n is the electron density) is related to the electric field via the magnetoconductivity tensor $\sigma(\boldsymbol{B})$ is given by

$$\sigma(\boldsymbol{B}) = \frac{ne^2\tau}{m*}\frac{1}{1+\omega_c^2\tau^2}\begin{pmatrix}1 & -\omega_c\tau\\ \omega_c\tau & 1\end{pmatrix}, \qquad (1.16)$$

Eq. (1.16) provides the magnetoconductivity for a spherical band with constant ($i.e.$ energy independent) relaxation time. From inversion of the matrix Eq. (1.16) we obtain the magnetoresistivity tensor

$$\rho(\boldsymbol{B}) = \frac{m*}{ne^2\tau}\begin{pmatrix}1 & w_c\tau\\ -w_c\tau & 1\end{pmatrix} \qquad (1.17)$$

From Eq. (17), we see that the diagonal (or parallel) magnetoresistivity $\rho_{xx}(\boldsymbol{B})$, the Hall magnetoresistivity $\rho_{yx}(\boldsymbol{B})$, and the Hall coefficient have the expressions

$$\rho_{xx}(\boldsymbol{B}) = \frac{m*}{ne^2\tau}, \quad \rho_{yx}(\boldsymbol{B}) = -\frac{\boldsymbol{B}}{nec}, \quad \boldsymbol{R}_{Hall}(\boldsymbol{B}) = -\frac{1}{nec}. \qquad (1.18)$$

We understand that in the spherical one band model with single relaxation time, the diagonal magnetoresistivity turns out to be independent from **B**, and we have $\rho_{xx}(\boldsymbol{B}) = \rho_{xx}(0) = \frac{m*}{ne^2\tau}$. Even more important, the Hall coefficient is independent both of the effective mass and the relaxation time; it depends only on the carrier concentration and charge sign. Also notice that in the case of positive holes, the off-diagonal matrix elements in Eq. (1.16) and Eq. (1.17) change sign.

1.1.2 Magneto transport, when the carrier in the crystal is an isotropic two-band model

The results that were obtained in Eq. 1.18 are to be taken only as idealized orientative, and cannot be used as they stand for quantitative descriptions of realistic conductors. It is important in fact to notice that a proper account of the energy of realistic conductor's dependence of the relaxation time, or of the anisotropy of the energy bands, modify the results of Eq. (1.18); in particular, a dependence of $\rho_{xx}(\boldsymbol{B})$ on $\boldsymbol{B}$ is actually always observed in experiments. For these reasons, we consider the slightly more sophisticated two-band model, representing two groups of carriers. For simplicity we suppose that the two bands are spherical. Let one band a material with n electrons of mass m_1 and relaxation time τ_1 and the other band is p hole of mass m_2 and relaxation time τ_2.

The magnetoconductivity is just the sum of the contributions from each group of carriers. Using Eq. (1.16) for electrons, and the appropriate modified form for positive holes, we obtain

$$\sigma(\boldsymbol{B}) = \begin{pmatrix}A_1 & -B_1\\ B_1 & A_1\end{pmatrix} + \begin{pmatrix}A_2 & B_2\\ -B_2 & A_2\end{pmatrix} = \begin{pmatrix}A_1+A_2 & -B_1+B_2\\ B_1+-B_2 & A_1+A_2\end{pmatrix}, \qquad (1.19)$$

where $A_1 = \frac{\sigma_1}{1+W_1{}^2\tau_1{}^2}$ $B_1 = \frac{\sigma_1 W_1\tau_1}{1+W_1{}^2\tau_1{}^2}$ $\sigma_1 = \frac{ne^2\tau_1}{m_1}$

$$A_2 = \frac{\sigma_2}{1+{w_2}^2{\tau_2}^2} \qquad B_2 = \frac{\sigma_2 w_2 \tau_2}{1+{w_2}^2{\tau_2}^2} \qquad \sigma_2 = \frac{pe^2\tau_2}{{m_2}^*}$$

The magnetoresistivity tensor is obtained by inverting the magnetoconductivity tensor Eq. (1.19); we have

$$\rho(\boldsymbol{B}) = \frac{1}{(A_1+A_2)^2+(B_1-B_2)^2}\begin{pmatrix} A_1+A_2 & -B_1+B_2 \\ -B_1+B_2 & A_1+A_2 \end{pmatrix}, \qquad (1.20)$$

We consider first the parallel component $\rho_{xx}(\boldsymbol{B})$ of the magnetoresistivity tensor of Eq. (1.20)

$$\rho_{xx}(\boldsymbol{B}) = \frac{\sigma_1+\sigma_2+\sigma_1{w_2}^2{\tau_2}^2+\sigma_2{w_1}^2{\tau_1}^2}{(\sigma_1+\sigma_2)^2+(\sigma_1 w_2\tau_2-\sigma_2 w_1\tau_1)^2}$$

It is straight forward to verify that $\rho_{xx}(\boldsymbol{B}) > \rho_{xx}(0)$; thus $\rho_{xx}(\boldsymbol{B})$- $\rho_{xx}(0)$ is an essentially positive quantity for any value of the magnetic field. We consider now the off-diagonal magnetoresistivity transport parameter $\rho_{yx}(\boldsymbol{B})$; from Eq. (1.20), we have

$$\rho_{yx}(\boldsymbol{B}) = \frac{-\sigma_1 w_1\tau_1(1+w_2^2\tau_2^2)+\sigma_2 w_2\tau_2(1+w_1^2\tau_1^2)}{(\sigma_1+\sigma_2)^2+(\sigma_1 w_2\tau_2-\sigma_2 w_1\tau_1)^2}$$

For high magnetic fields ($i.e.\ w_i\tau_i >> 1$), the above expression simplifies in the form

$$\rho_{yx}(\boldsymbol{B}\to\infty) \approx \frac{w_1\tau_1 w_2\tau_2}{\sigma_1 w_2\tau_2-\sigma_2 w_1\tau_1} = -\frac{\boldsymbol{B}}{(n-p)ec}, \qquad (1.21)$$

Finally hall parameter become

$$R_{Hall}(\boldsymbol{B}\to\infty) = -\frac{1}{(n-p)ec}, \qquad (1.22)$$

Thus Hall coefficient in a case of two types of carriers, it is independent on relaxation time and is governed by the difference of the density of electrons and holes.

CHAPTER TWO

Two-dimensional electron systems

A two-dimensional electron gas can be realized at the surface of a semiconductors like silicon or gallium arsenide where the surface is usually in contact with a material which act as insulator(SiO_2 for silicon effect transistor and for example $Al_xGa_{1-x}As$ for heterostructure)[5].

As electrons are restricted to move only in two dimensions, their behavior is bound to be different than in three-dimensional systems, for instance, as Landau pointed out, the motion in a plane perpendicular to a uniform magnetic field has discrete energy levels, called Landau levels(LL).

2. 1 Landau quantization

We start by considering the quantum mechanical problem of motion of a single electron in two dimensions in a homogeneous magnetic field directed perpendicular to the plane. The Hamiltonian for a single electron in the electromagnetic field is given by[6]

$$H= \frac{1}{2m}\{\boldsymbol{P}+\frac{e}{C}\boldsymbol{A}\}^2 = \frac{[P_x+\frac{e}{C}A_x]^2+[P_y+\frac{e}{C}A_y]^2}{2m}, \quad (2.1)$$

where **A** is the vector potential of the magnetic field, and $\boldsymbol{P}= -i\hbar\nabla$ is the momentum operator. It is useful to choose the so called Landau gauge for the vector potential of the homogeneous magnetic field directed along z-axis

$$\boldsymbol{A}_x = -\boldsymbol{B}y;\ \boldsymbol{A}_y = 0, \quad (2.2)$$

where **B** is the magnitude of the field. Substituting this equation in Eq. (2.1) we find that

$$H = \frac{[P_x-\frac{e\boldsymbol{B}y}{c}]^2+P_y]^2}{2m}$$

$$= \frac{[-i\hbar\partial_x-\frac{eBy}{c}]^2}{2m}-\frac{\hbar^2\partial_y^2}{2m}$$

So that the Schrödinger equation has the following form

$$H\,\Psi_{(x,y)} = E\Psi_{(x,y)}$$

$$\{\frac{[-i\hbar\partial_x-\frac{eBy}{c}]^2}{2m}-\frac{\hbar^2\partial_y^2}{2m}\}\Psi_{(x,y)} = E\Psi_{(x,y)}, \quad (2.3)$$

The differential operator on the left hand side of Eq. (2.3) is translationary invariant in the x-direction, so that one can use the wave function of the following form

$$\Psi_{(x,y)} = e^{ikx}\phi(y), \tag{2.4}$$

Substituting this equation in Eq. (2.3) we get

$$\{\frac{(\hbar k-\frac{eBy}{c})^2}{2m} - \frac{\hbar^2\partial_y^2}{2m}\}\phi(y) = E\phi(y), \tag{2.5}$$

One can easily see that this is nothing but the Schrödinger equation for the harmonic oscillator, whose equilibrium position y_0 and the frequency ω_c are given by: $y_0 = \frac{\hbar ck}{eB}$; $\omega_c = \frac{eB}{mc}$ respectively. Thus we conclude that the energy levels for the electron in the magnetic field, the so called Landau levels, are given by the expression

$$E_n = \hbar\omega_c(n + \frac{1}{2}), \tag{2.6}$$

where n is a positive integer number. Importantly, these energies are independent of quantum number k, which implies a strong degeneracy.

In the absence of a magnetic field, the density of states (DOS) in 2D is constant as a function of energy. With a magnetic field turned on however, the density of states collapses onto a series of highly degenerate δ-functions (in the ideal, zero disorder case), corresponding to the Landau Levels. In real samples, the δ-functions are broadened due to disorder scattering. The LL degeneracy, $i.e.$ the number of states per LL (per unit area) varies with the size of the $\boldsymbol{B}$ field according to

$$n_{\boldsymbol{B}} = \frac{e\boldsymbol{B}}{h}, \tag{2.7}$$

Where the spin degeneracy has not been included, which, for spin degenerate system would contribute an additional factor of two. As the magnetic field is increased, the degeneracy of the LLs, or in other words the size of the LLs (in k-space), increases so that it requires more electrons to fill up each LL. At very low temperatures, electrons fill the lowest available energy states in the usual way so that LLs are filled sequentially up to the Fermi level. At low temperatures and low magnetic fields a large number of LLs will in general be filled.

As the magnetic field is increased the LL degeneracy increases resulting in fewer and fewer LLs being occupied until at sufficiently large values of $\boldsymbol{B}$ only the lowest LL contains any electrons. Between these two extremes there exists special cases where an integer number of LLs are exactly filled, occurring at magnetic field values of

$$\boldsymbol{B}_{\nu} = \frac{1}{\nu}\frac{nh}{e}, \tag{2.8}$$

where $\nu = \frac{n}{n_{\boldsymbol{B}}}$ is termed the filling fraction. The filling fraction gives the ratio between the number of electrons and the number of available states per LL. For example $\nu = 1$ indicates the lower spin branch of the lowest LL ($n = 0$) is exactly filled; $\nu = \frac{3}{2}(= 1 + \frac{1}{2})$ indicates the lower spin branch of the lowest LL is completely filled plus exactly half of the upper spin branch in the lowest LL is filled, while at $\nu = 2$ both spin branches of the L level are exactly filled, and so on.

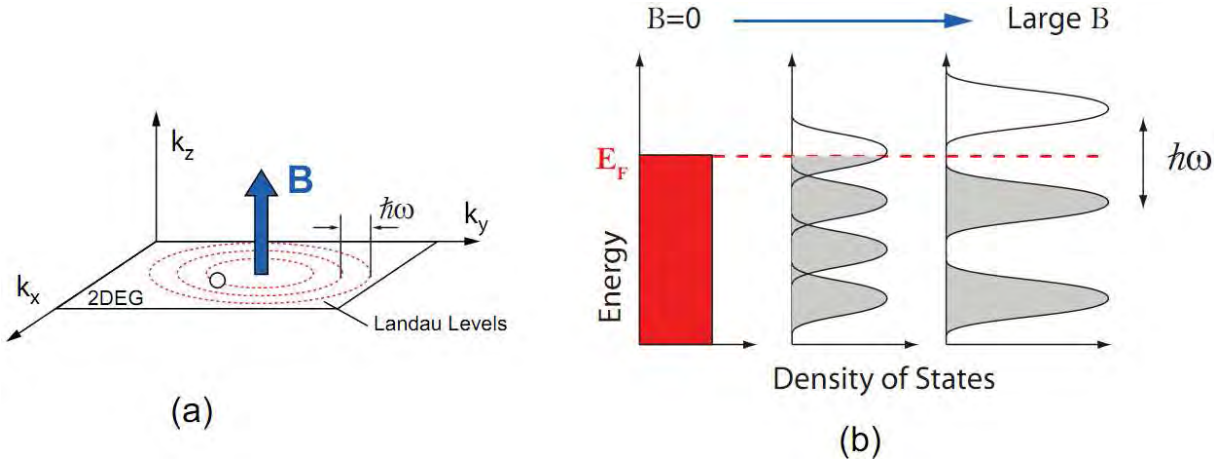

Figure 2.1: (a) Application of a magnetic field causes the electron energy states to collapse onto concentric circular orbits (in k-space), separated by a well defined gap. (b) Increasing the magnetic field increases the size of the LLs so that fewer and fewer LLs are occupied if the electron density remains fixed. At special values of the $\boldsymbol{B}$ field (far right panel) an integer number of LLs are exactly filled, and the Fermi level lies in the gap between adjacent LLs. The LLs are shown as disorder broadened, rather than as ideal (unrealistic) δ-functions in the DOS.

It is useful to note that there are several equivalent definitions of the filling fraction

$$\nu = \frac{n}{n_{\boldsymbol{B}}} = \frac{nh}{e\boldsymbol{B}} = \frac{\Phi_o}{\boldsymbol{B}} = n2\pi l_{\boldsymbol{B}}^2, \tag{2.9}$$

which can all be derived from the above equations, where $\Phi_o = \frac{h}{e}$ is the definition of the flux quantum, and $2\pi l_B^2$ is simply the area of a Landau level whose radius is the magnetic length, $l_{\boldsymbol{B}} = \sqrt{\frac{\hbar}{eB}}$, density per unity area is, $n_{\mathbf{B}} = \frac{1}{2\pi l_{\boldsymbol{B}}^2}$. In particular, it can be illuminating to note that from the definition of the flux quantum, the LL degeneracy (per unit area)in Eq. (2.7) can be rewritten as $n_{\mathbf{B}} = \frac{\boldsymbol{B}}{\Phi_0}$. For a sample of area A, this gives the total number of states per LL to be

$$N_{\mathbf{B}} = \frac{A\boldsymbol{B}}{\Phi_o} = \frac{\Phi}{\Phi_o}, \tag{2.10}$$

where Φ is the total flux penetrating the sample. Rewriting the LL degeneracy in this way reveals explicitly that there exists one energy state for each quantum of flux that penetrates the sample. At exact filling, all lower energy states (LLs) are completely filled while the higher levels are separated by the energy gap between LLs ($i.e.$ the cyclotron energy gap, $\Delta = \hbar\omega_c$). Since there are no free energy states within the filled LL level there can be no scattering as there are no available states to scatter into, provided the temperature is low enough that $k_B T < \Delta$. The transport therefore becomes dissipationless and the resistance falls to zero. Recall from the classical Hall effect, that the Hall resistance is $R_H = \frac{B}{ne}$. Substituting into this relation the result from Eq. 2.8, therefore gives the value of the Hall resistance at the condition of exact LL filling to be

$$R_H = \frac{1}{\nu}\frac{h}{e^2}, \tag{2.11}$$

which is exactly the quantized resistance values of the plateaus observed in experiment.

2.2 Creation of a two-dimensional electron system

Constructing a 2DES can be done in a three-dimensional materials with confining electrons to the interface between two substances, thus restricting electron movement in direction perpendicular to the interface[2]. The QHE was discovered in a 2DES where electrons were confined to the interface between two different semiconductors. While Klitzing et al. used the Si MOSFET to create a 2DES, Störmer, Tsui, and Gossard did this at a GaAs/AlGaAs heterojunction obtaining much higher mobilities of the electrons. Both types of 2DES are schematically shown in $Figure$ 2.2. They used samples consisting of undoped GaAs, undoped $Al_{0.3}Ga_{0.7}As$, Si-doped $Al_{0.3}Ga_{0.7}As$, and Si-doped GaAs single crystals, each around 500 Å thick, sequentially grown on GaAs substrates using molecular beam epitaxy techniques, which are high-vacuum evaporation techniques allowing building up solids one layer at a time.

GaAs and AlGaAs interfaces are frequently used as there is nearly no lattice distortion incurred by placing layers of GaAs and AlGaAs together. This is due to GaAs and AlAs having very similar crystal structure, with lattice constants of 5.63 Å and 5.62 Å respectively and both adopting the zincblende structure, therefore by replacing some gallium atoms with aluminium ones lattices change negligibly.

Gap energies for $Al_{0.3}Ga_{0.7}As$ and GaAs differ and give rise to band bending at the junction between $Al_{0.3}Ga_{0.7}As$ and GaAs layers as shown in $Figure$ 2.3(A). When doping of both sides of the junction is heavy enough, chemical potential μ can rise above the notch in the potential, thus creating a small region, occupied even at zero temperature, called inversion layer, as shown in $Figure$ 2.3(C). The notch in the potential can be also interpreted to present a one-dimensional attractive triangular potential for electrons, always having at least one bound

eigenstate. The potential barriers in the vicinity of heterojunction are on the order of 0.1 eV, thus restricting the temperatures to a few kelvin or less, if only the ground state was to have significant occupation.

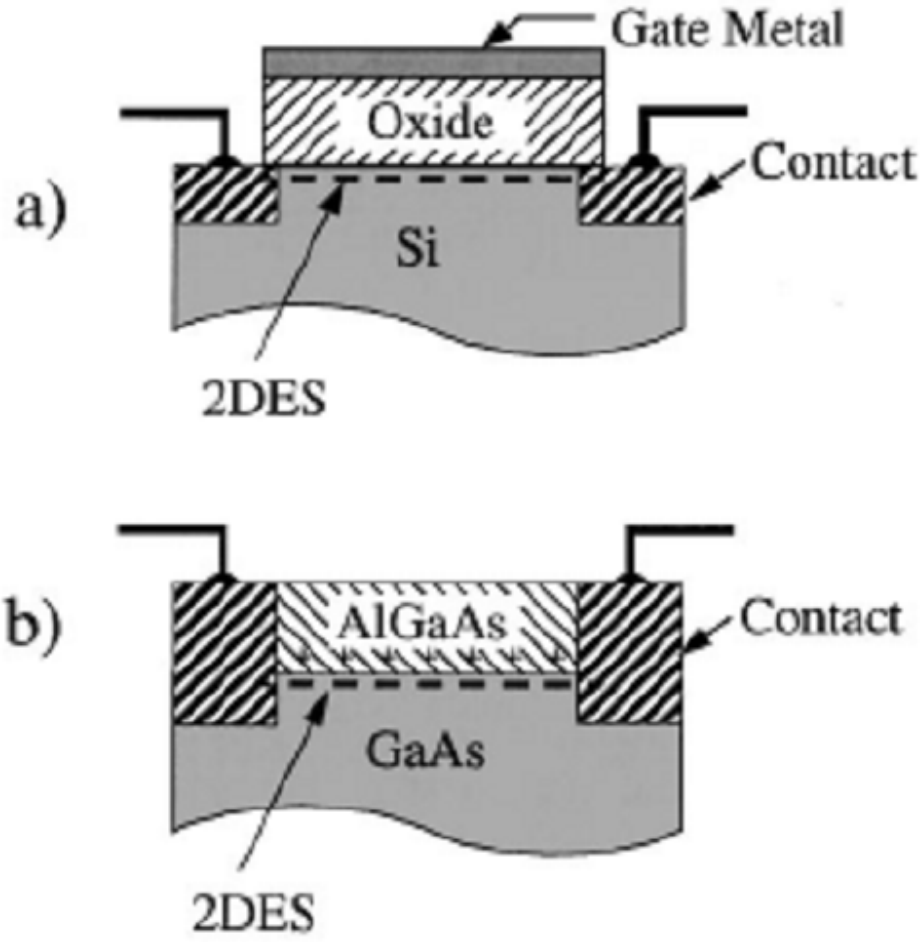

Figure 2.2: Schematic drawings of a two dimensional electron gas in (a) a silicon MOSFET transistor and (b) a GaAs/AlGaAs heterojunction

By creating a heterojunction between $Al_{0.3}Ga_{0.7}As$ and GaAs and keeping the temperature low enough, the electrons are trapped in the one-dimensional triangular potential, thus being confined to the interface between semiconductors and giving rise to a two-dimensional electron gas.

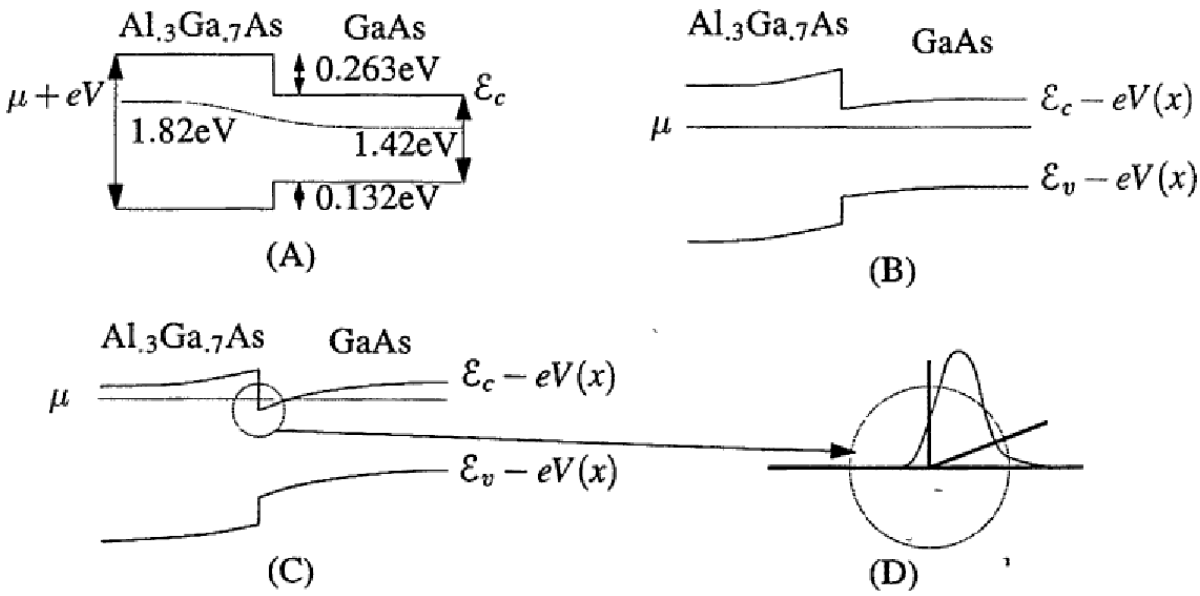

Figure 2.3: (A) and (B) schematic picture of junction between $Al_{0.3}Ga_{0.7}As$ and GaAs semiconductors. (C) In case of heavy doping chemical potential μ can rise above conduction band edge, which is enlarged in (D), where a bound-state wave function is sketched. The junction plane is projected to one dimension for better clarity.

Electron scattering is undesirable, as it obscures the mutual electron interactions and interactions with the magnetic field. Scattering occurs on impurities, such as lattice distortions, impurities introduced with doping, and on phonons. The latter part of scattering can readily be minimized by cooling the sample, while the former part can be taken care of with appropriate choice of materials. As the heterojunction mentioned above has very small lattice distortions, only scattering on doped impurities needs to be prevented. This is done by introducing the doped Si atoms around 0.1 μm away from the interface between $Al_{0.3}Ga_{0.7}As$ and GaAs semiconductors. This distance assures little scattering as well as transfer of electrons to inversion layer.

The quality of samples containing 2DESs is usually described with electron mobility. Bulk GaAs has a mobility of the order of $10^3 cm^2/Vsec$, while recent doped samples achieved mobilities on the order of $10^7 cm^2/Vsec$ at temperatures around 1K. For illustration, mobility of $2x10^7 cm^2/Vsec$ corresponds to approximately 0.2 mm mean free path.

CHAPTER THREE

The quantum Hall effect

The quantum Hall effect (QHE) is one of the most remarkable condensed-matter phenomena discovered in the second half of the 20th century.

In 1980, performing a similar experiment to Edwin Hall's but in the quantum regime (very low temperature, high magnetic field and in the 2D limit), Klaus von Klitzing discovered the quantum Hall effect[7].

In von Klitzing's experiment, shown in $Fig.3.1$, the basic Hall effect was observed, namely the Hall resistance varies with magnetic field, however at well defined values of field $\boldsymbol{B}$, plateaus appear in the Hall resistance, together with vanishing resistance measured in the longitudinal direction.

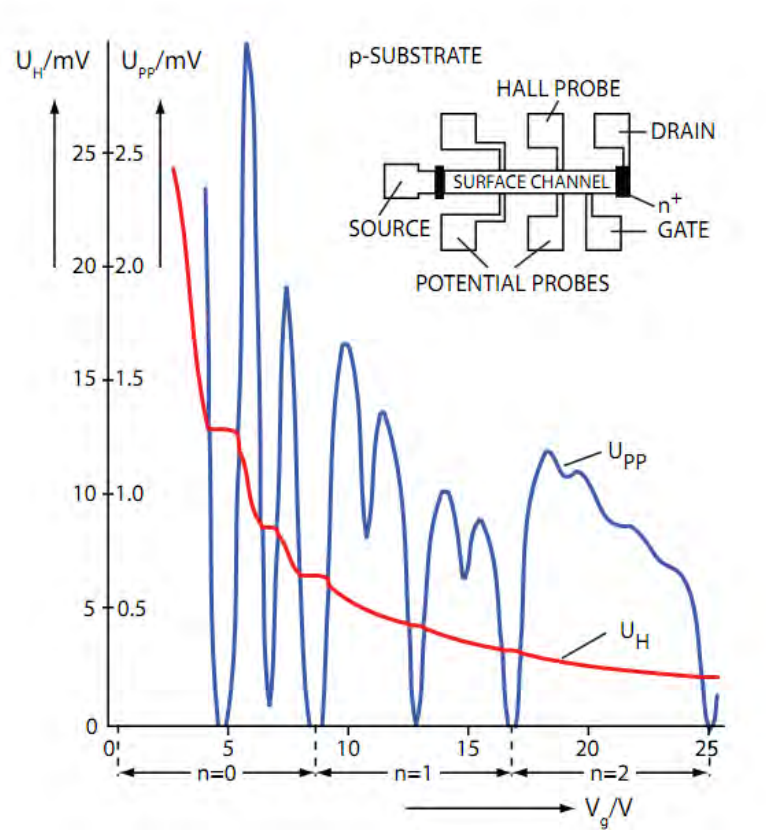

$Figure$ 3.1: Plot from von Klitzing's discovery of the quantum Hall effect. Plateaus in the Hall resistance were observed to be quantized to integer multiples of $\frac{h}{e^2}$, together with vanishing resistance in the longitudinal direction. Experimental results for the Hall voltage U_H and the longitudinal voltage U_{PP} at T = 1.5 K and B = 18 T as a function of the gate voltage V_g which is directly related to the carrier density n. The inset shows a top view of the device with dimensions 400 × 50 μm

When strong magnetic field is applied perpendicular to the two dimensional conductors, let say 2DES, at low temperature, conductivity is quantized. $i.e$

$$\sigma_{xy} = \frac{ve^2}{h}, \tag{3.1a}$$

and the diagonal conductivity vanishs.

$$(\sigma_{xx} = 0 \text{ or } \sigma_{yy} = 0), \tag{3.1b}$$

where v is rational number. This phenomenon is called the quantum Hall effect.

When v in Eq. (3.1a) is an integer we get integer quantum Hall effect and when $v = \frac{p}{q}$ and p and q are relatively prime integers, it is corresponding to fractional quantum Hall effect[8].

The transport properties of two-dimensional conductors, when observed in highly purity sample, at very low temperature and strong magnetic field, show departure from classical behavior; in particular the hall resistance ρ_{xy}(B) versus B exhibits flat plateaus from which the universal constant $\frac{h}{e^2}$ can be obtained. Very accurate measurements performed on two-dimensional electron gases have given the value of $\frac{h}{e^2}$ [9].

$$\frac{h}{e^2} = 25812.806\Omega = \frac{2\pi}{sc\alpha}, \tag{3.2}$$

where $sc\alpha$ is fine structure constant of two dimensional system.

With an error less than one part per million or the quantization is accurate to a few parts in 10^8 making this one of the most precise measurements of the fine structure constant,

$$\alpha = \frac{e^2}{c\hbar}, \tag{3.3}$$

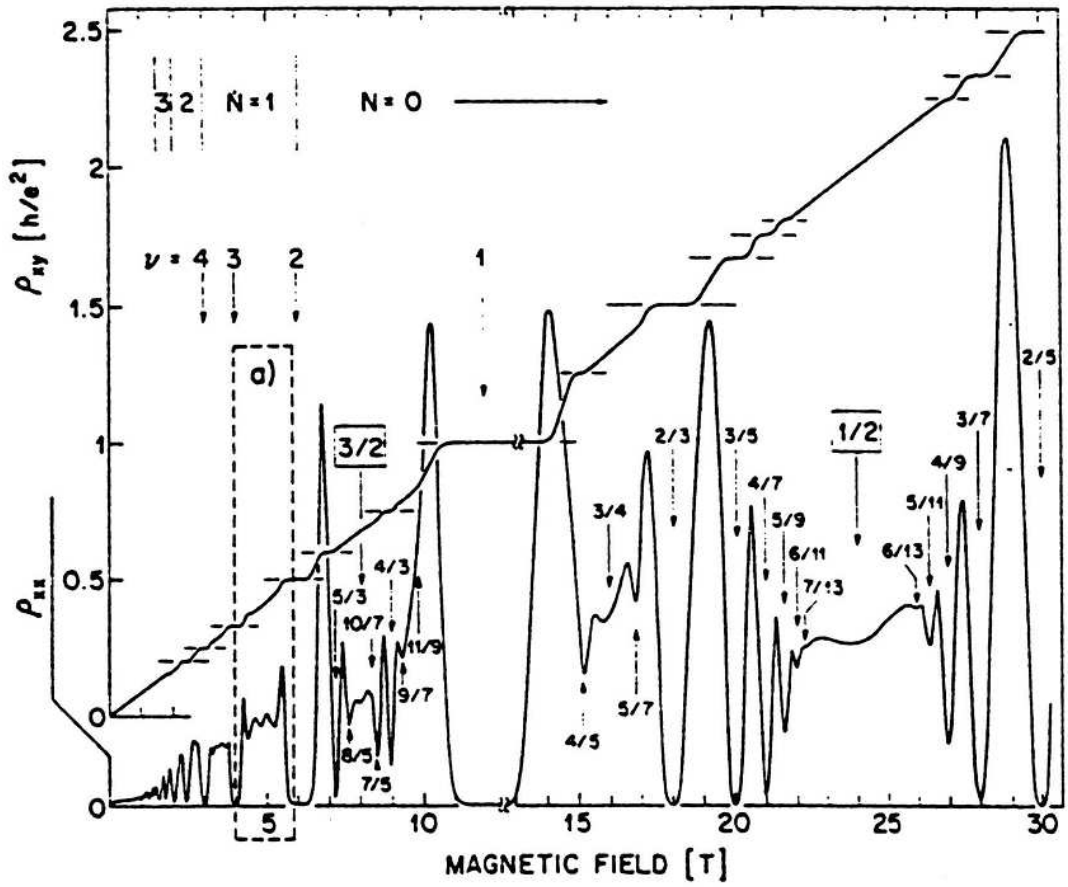

Figure 3.2: ρ_{xx} and ρ_{yx} vs. magnetic field, B, in the quantum Hall regime. A number of integer and fractional plateaus can be clearly seen. This data was taken at Princeton on a GaAs-AlGaAs heterostructure.

For a qualitative understanding of some features of the quantum Hall effect, it is convenient to examine first the Hall effect within a classical modelistic point of view; later we introduce heuristically the effect of quantization.

Consider a two-dimensional electron system (in the xy plane) in the presence of a strong perpendicular magnetic field. Let n_s denote the surface carrier density.

Similarly, let $\boldsymbol{J}^{(\text{surf})} = n_s(-e)\boldsymbol{v}$ denote the surface current density. In the presence of a magnetic field, carriers are deflected and in general $\boldsymbol{J}^{(\text{surf})}$ is no more parallel to the electric field (in the xy plane); rather we have

$$J_i^{surf} = \sum_j \sigma_{ij}(\mathbf{B})\mathbf{E}_j, \tag{3.4a}$$

$$\mathbf{E}_i = \sum_j \rho_{ij}(\boldsymbol{B}) J_j^{surf}, \tag{3.4b}$$

In the standard geometry of $Fig.1$

$$\rho_{yx}(\boldsymbol{B}) = \frac{\boldsymbol{E}_y}{\boldsymbol{J}_x^{surf}} = \frac{\boldsymbol{E}_y\, d_y}{\boldsymbol{J}_x^{surf} d_y} = \frac{\boldsymbol{V}_{Hall}}{I_x}, \tag{3.5}$$

Thus we see that for the two-dimensional system the Hall resistance $\rho_{yx}(\boldsymbol{B})$ is given by the Hall voltage divided by the current flowing in the sample; $\rho_{yx}(\boldsymbol{B})$ can thus be measured with high accuracy, since the precise sample dimensions are not relevant and tend to drop out.

The magnetoconductance of a two-dimensional electron system in a modelistic approach with constant relaxation time, is given by Eq. (1.16), once n is replaced by n_s; we have

$$\sigma(\boldsymbol{B}) = \frac{n_s e^2 \tau}{m*} \frac{1}{1+\omega_c^2\tau^2} \begin{pmatrix} 1 & -\omega_c\tau \\ \omega_c\tau & 1 \end{pmatrix}, \tag{3.6}$$

In the idea collisionless regime, taking the limit τ—>∞ of expression Eq. (3.6), we obtain

$$\sigma(\boldsymbol{B}) = \frac{n_s ec}{\boldsymbol{B}} \begin{pmatrix} 0 & -1 \\ 1 & 0 \end{pmatrix}, \tag{3.7}$$

from Eq. (3.7), valid in the absence of scattering events, we see that the diagonal Conductance $\sigma_{xx}(\boldsymbol{B})$ is zero and the Hall conductance $\sigma_{xy}(\boldsymbol{B}) = -\frac{n_s ec}{\boldsymbol{B}}$ is inversely proportional to $\boldsymbol{B}$. From Eq. $(3.4a)$ and $Eq.(3.7)$, in the standard geometry of $Fig.1$, we have $\boldsymbol{E}_x = 0$ and $\boldsymbol{J}_x^{surf} = -\left(\frac{n_s ec}{\boldsymbol{B}}\right)\boldsymbol{E}_y$. Thus a current flows in the x-direction with null electric field in the x-direction; the current $\boldsymbol{J}_x^{surf}$ is driven by the transverse electric field $\boldsymbol{E}_y$, acting in conjunction with the perpendicular magnetic field $\boldsymbol{B}$.

From inversion of the magnetoconductance matrix $(Eq.3.7)$, the magnetoresistance matrix in the ideal collisionless regime is given by

$$\rho(\boldsymbol{B}) = \frac{\boldsymbol{B}}{n_c ec} \begin{pmatrix} 0 & 1 \\ -1 & 0 \end{pmatrix}, \tag{3.8}$$

Thus, for the two-dimensional electron gas in the absence of scattering, the classical Hall resistance $\rho_{xy}(\boldsymbol{B}) = \frac{\boldsymbol{B}}{n_c ec}$ is linear in $\boldsymbol{B}$, and the diagonal resistance $\rho_{xx}(\boldsymbol{B})$ is always zero.

We can reasonably argue that the condition of collisionless regime holds at those very values of the magnetic field, for which Landau levels are either fully occupied or completely empty. In fact, in this situation, electrons cannot suffer either elastic or quasi-elastic scattering events (at low temperatures), because energy gap of the order of $\hbar\omega_c$ or $\mu_B \boldsymbol{B}$ separates occupied states from empty states.

CHAPTER FOUR

The Integer Quantum Hall Effect

In 1980 Klitzing et al. discovered the so called integer quantum Hall effect (IQHE) in which the quantum number ν in a quantized conductivity(i.e $\sigma(\boldsymbol{B}) = \frac{\nu e^2}{h}$) is a simple integer.

The IQHE effect can be largely understood in terms of the properties of non-interacting electrons whose energy eigenvalues in the absence of disorder are the Landau levels (LL), $E = \hbar w_c(n+\frac{1}{2})$. This means the integer quantum Hall effect occurs in the regime in which impurities dominate[7].

In this section we will mention two separate arguments for the QHE, namely Laughlin's gedanken-experiment, which essentially builds upon gauge invariance as a fundamental principle in Nature, and B$\ddot{u}$ttiker's theory of edge currents.

4.1 Laughlin's Gendanken-Experiment

Let us now consider the argument for the integer QHE proposed by R. B. Laughlin, which essentially is based on gauge invariance as a fundamental principle in Nature.

The Gedanken-experiment is based on the setup shown in $Fig.4.1$. The 2D xy-surface, to which the electrons are confined is rolled up into a cylinder with radius R, which encloses a magnetic flux Φ oriented along the z-direction[4]. Further, a constant applied magnetic field $\boldsymbol{B}$ penetrates the cylindrical surface. In a local cartesian coordinate system we can describe the applied field $\boldsymbol{B}$ in the Landau gauge by the vector potential adopted from, A_{app}= (0, $\boldsymbol{B}_{r_x}$, 0). To describe the magnetic flux Φ, we write[10,11,12]

$$\Phi = \int_s \boldsymbol{B}.da = \int_s \nabla x \boldsymbol{A}_\Phi.da = \oint_{\delta s} \boldsymbol{A}_\Phi.dl = (\boldsymbol{A}_\Phi)_y 2\pi R \qquad (4.1)$$

where s is a surface which is penetrated by the flux Φ. The corresponding vector potential can thus be written as $\boldsymbol{A}_\Phi$= (0, $\frac{\Phi}{2\pi R}$, 0).

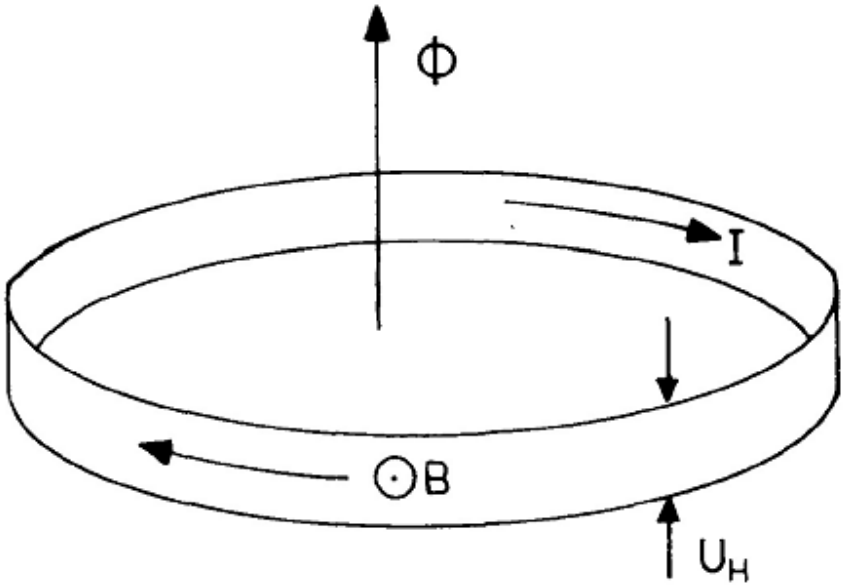

Figure 4.1: Setup used for Laughlin's gedanken-experiment.

Now, what happens to the electronic wave functions Ψ, If we change the flux by $\Phi \rightarrow \Phi' = \Phi + \Delta\Phi$? Changing flux is kind of gauge transformation which causes a phase shift of wave function. The magnetic field seen by the electrons on the 2D surface is unchanged, but the total vector potential will change as $\boldsymbol{A}_{tot} \rightarrow \boldsymbol{A}'_{tot} = \boldsymbol{A}_{tot} + (0, \frac{\Delta\Phi}{2\pi R}, 0)$. Remember that Schrodinger's equation is unchanged by a gauge transformation,

$$\boldsymbol{A} \rightarrow \boldsymbol{A}' = \boldsymbol{A} + \nabla\chi, \quad \Phi \rightarrow \Phi' = \Phi - \frac{\partial\chi}{\partial t}, \quad \Psi \rightarrow \Psi' = \Psi e^{-ie\chi/\hbar} \tag{4.2}$$

where $\chi = \chi(r,t)$ is an arbitrary smooth, real scalar function. Thus, if we write

$$\chi(r,t) = r_y \frac{\Delta\Phi}{2\pi R}, \tag{4.3}$$

we see that the change of flux should be equivalent to a gauge transformation by χ, which only affects the phase of the wave function. However, since the electron system is not simply connected in the cylinder geometry, we need to consider the Aharonov–Bohm effect and pay special attention to the boundary conditions (BC) of the wave functions.

There are two generic possibilities:

(i) When the region where the wave function Ψ is finite does not extend all the way around the cylinder – $i.e.$ that it is localized in the y-direction – the relevant BC along y is just that the wave function has to vanish. For this category of electronic wave functions any gauge transformation is thus permitted by the BC.

(ii)When the wave function Ψ is extended all the way around the cylinder – i.e. that it is delocalized – it has to fulfill periodic BC's, $\Psi(r_x, r_y + 2\pi R) = \Psi(r_x, r_y)$. Therefore, also the gauge transformed wave functions has to be periodic,

$$e^{\frac{ie\chi(r_x, r_y+2\pi R)}{\hbar}} = e^{\frac{ie\chi(r_x, r_y)}{\hbar}} \tag{4.4}$$

With the use of Eq. (4.3) the above reduces to $e^{\frac{ie\Delta\Phi}{\hbar}} = 1$, or to the criterium.

$$\Delta\,\Phi = \Phi_0 \times \text{integer}, \tag{4.5}$$

where $\Phi_0 \equiv \frac{h}{e}$ the flux quantum. Therefore, a continuous gauge transformation is forbidden for the extended states.

From this observation another question arises: What happens to the extended states when the flux Φ is continuously changed and a gauge transformation cannot generally be invoked. The total vector potential can be written as

$$\boldsymbol{A}_{tot} = \{0, (r_x + \frac{\Phi}{2\pi \mathrm{R}}), 0\}, \tag{4.6}$$

from which we see that a flux change $\Delta\Phi$ is equivalent to a mechanical translation $\Delta r_x, = \frac{\Delta\Phi}{2\pi R\boldsymbol{B}}$ in the x-direction of the extended states. When $\Delta\,\Phi = \Phi_0$ all the extended states should be identical to the initial states, since here a gauge transformation can be applied. But, focusing on a finite piece of the cylinder, it is evident that the continuous flux change from zero to $\Delta\Phi = \Phi_0$ has effectively resulted in the transfer of one electron (per filled band) from one edge to the other. This action thus works like a conveyor belt.

The energy associated with this transport can be written as; $\Delta E = \nu e U_H$, where ν is the number of filled bands and U_H is the Hall voltage between the edges of the cylinder. Finally, Under the condition of vanishing conductivity σ_{xx} (no energy dissipation) energy is conserved and one can write Faraday's law of induction in a form which relates the current I in the loop to the total energy of the system E with respect to the magnetic flux Φ threading the loop

$$I = \frac{\partial E}{\partial \Phi}, \tag{4.7a}$$

Thus, Faraday's law of induction the current density along y is just

$$\boldsymbol{J_y} = \frac{1}{L_x}.\frac{\partial E}{\partial \Phi} = \nu e^2 \frac{U_H}{hL_x} = E_x \nu \frac{e^2}{h} \tag{4.7b}$$

and hence the Hall resistivity assumes the quantized

$$\rho_{xy} = \frac{h}{\nu e^2} \tag{4.8}$$

Where, ν = 1, 2, 3,. . . characteristic of QHE .

Again, also Laughlin's gedanken-experiment assumes the existence of extended states in order to describe the QHE. Within his picture the reason for QHE is thus the flux quantization Φ_0 and the quantization of charge into elementary charges e.

4. 2 Büttiker's Theory of Edge Currents

Another way to obtain the quantized conductivity of QHE is to use the Landauer- Büttiker formalism. The theoretical framework commonly used to describe transport through conductor so called mesoscopic devices is the Landauer-Büttiker approach. In this topic we will give a review of this approach and see how current can be described in terms of transmission probabilities[10,11,12].

The standard setup for the theory consists of a mesoscopic device connected to electron reservoirs via leads ($see\ Fig.\ 4.2$). The reservoirs provide thermalized electrons to occupy the states of the leads. The contacts between leads and reservoirs are considered to be reflectionless, so that electrons coming from the leads can enter the reservoir without suffering reflections, and are thermalized before being re-emitted.

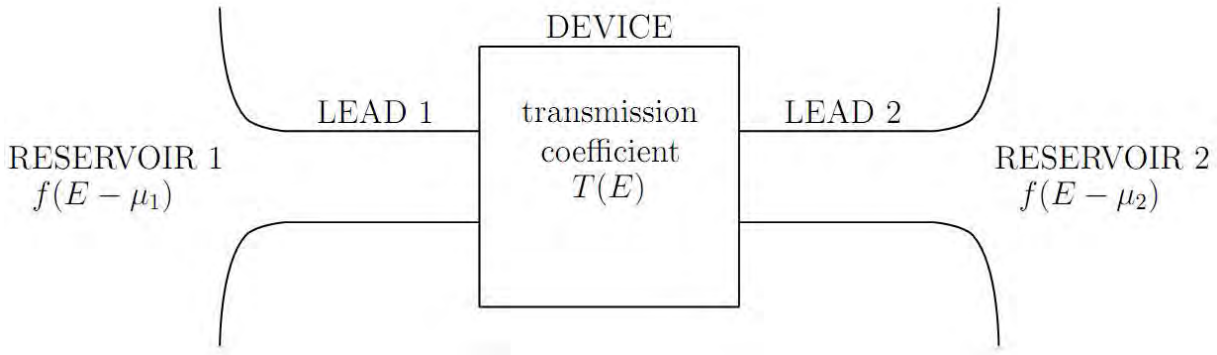

$Figure\ 4.2$: Typical setup for the Landauer-Büttiker formalism. Two reservoirs are connected via leads to a mesoscopic device with transmission coefficient T(E).

Furthermore, the leads are considered perfect, i.e. they are translational invariant in the propagating direction. The finite width in the transverse direction however leads to a quantized transverse modes. The wavefunctions in the leads are thus of the form $e^{ikx}\varphi_n(y)$. The transverse modes $\varphi_n(y)$ are also referred to as eigenchannels.

The conductance through the sample can now be expressed in terms of transmission probabilities T_n, i.e., the probability for an electron in channel n to be transmitted through the sample. The result is the Landauer formula [10, 11, 12];

$$G = \frac{2e^2}{h}\sum_n T_n(E_F), \tag{4.9}$$

where G is quantized conductivity through mesoscopic devices.

We will now give a heuristic, intuitive derivation of the Landauer formula.

The population of the states in the leads is given by the Fermi-Dirac distribution $f(E-\mu_\alpha)$ where μ_α is the chemical potential of the reservoir α = 1, 2. The electrical current originating from electrons in lead α carried by channel n is given by

$$I_{\alpha nE} = \frac{2e}{L}\sum_k T_n(E)\boldsymbol{v}(k)f(E-\mu_\alpha), \quad \alpha = 1, 2\ldots \tag{4.10}$$

where L is the length of the device. The factor 2 accounts for the spin, $\boldsymbol{v}(k)$ is the group velocity of the electrons and $T_n(E)$ gives the transmission probability of channel n at energy $E(k)$. The net current is obtained by calculating the difference between the currents originating from the two leads, and summing over all quantum channels

$$I = \sum_n I_{1nE} - I_{2nE}, \tag{4.11a}$$

$$= \frac{2e}{L}\sum_{n,k} v(k)T_n(E)\{f(E-\mu_1)\text{-}f(E-\mu_2)\}, \tag{4.11b}$$

The current is taken positive when flowing from the lead to the device. Converting the sum over the momentum k into an integral according to the usual rule

$$\sum_k \quad \rightarrow \frac{L}{2\pi}\int dk\,, \tag{4.12}$$

and using the relation

$$v(k) = \frac{1}{\hbar}\frac{dE}{dk}, \tag{4.13}$$

we find

$$I = \frac{2e}{h}\sum_n \int dE\, T_n(E)\{f(E-\mu_1) - f(E-\mu_2)\}, \tag{4.14}$$

At low temperatures and for low voltages $eV = \mu_1 - \mu_2$, we can make a Taylor expansion of $f(E-\mu_1)-f(E-\mu_2)$ around the Fermi energy, which leads to $f(E-\mu_1)-f(E-\mu_2) \approx \delta(E-E_F)(\mu_1 - \mu_2)$. Inserting this in Eq. (4.14), one obtains for the conductance through the system

$$G = \frac{2e^2}{h}\sum_n T_n(E_F) \equiv \frac{2e^2}{h}.T(E_F) \quad (4.15)$$

where we defined the total transmission coefficient $T(E_F)$ as the sum of all transmission probabilities $T_n(E_F)$. The previous discussion can straightforwardly be extended to systems with more than two leads. In that case, a sum over all leads (indexed by α and β) has to be taken. The total current through lead α is then given by

$$I_\alpha = \frac{2e}{h}\sum_{\beta\neq\alpha}\{T_{\beta\alpha}(E_F)\mu_\alpha - T_{\alpha\beta}(E_F)\mu_\beta\}, \quad (4.16)$$

where $T_{\beta\alpha}(E_F)$ is the total transmission coefficient from lead α to lead β. We can rewrite this expression with $V_\mu = \frac{\mu_\alpha}{e}$

$$I_\alpha = \sum_\beta\{G_{\beta\alpha}V_\alpha - G_{\alpha\beta}V_\beta\}, \quad (4.17)$$

where the conductances

$$G_{\alpha\beta} = \frac{2e^2}{h}T_{\alpha\beta}(E_F), \quad (4.18)$$

describe the conductance between the different leads. From a physical point of view we need to ensure current conservation and gauge invariance. Current conservation implies for a multiterminal geometry that $\sum_\alpha I_\alpha = 0$. The gauge invariance means that no current arises when all chemical potentials are shifted by the same value. These two physical considerations lead to the following property

$$\sum_\alpha G_{\alpha\beta} = \sum_\beta G_{\alpha\beta} = 0, \quad (4.19)$$

We can then rewrite Eq. (4.17)

$$I_\alpha = \sum_\beta G_{\alpha\beta}(E)\{V_\alpha - V_\beta\}, \quad (4.19)$$

Calculating transport properties of a mesoscopic device thus essentially comes down to calculating transmission coefficients.

Thus, for a macroscopic sample where the scattering probability from one edge to the other is extremely small, the current will hence flow without resistance along the edges, $i.e.$ $\rho_{yy} = 0$, even when the sample is disordered and contain impurities! Also, with exactly one forward propagating state and one backward propagating state per Landau level (per volume) at the Fermi level we see from the Landauer- Büttiker formula $Eq.(4.9)$ that the Hall resistivity is quantized $\rho_{xy} = \frac{h}{\nu e^2}$, where ν is the number of filled of Landau level[10].

CHAPTER FIVE

The Fractional quantum Hall effect

The fractional quantum Hall effect (FQHE) was discovered in 1982 by Tsui, St*ö*rmer and Gossard by their experiments that were performed on two dimensional electron systems at the interface of GaAs/AlGaAs heterostructures at even lower temperatures and higher magnetic fields**.** These systems allow for higher electron mobilities due to modulation doping which removes the defects from the plane of the two-dimensional electron system. In their article[13] Tsui, St*ö*rmer, and Gossard reported "some striking, new results on the transport of high-mobility, 2D electrons, in GaAs-AlGaAs heterojunctions in the extreme quantum limit, when the lowest-energy, spin-polarized Landau level is partially filled". The striking result was a dip in the diagonal part of the resistivity tensor ρ_{xx} and a plateau in Hall resistivity ρ_{xy} at the $\frac{1}{3}$ filling factor of the first Landau level. Integer quantum Hall effect, discovered some time before Tsui, Stormer and Gossard conducted their experiment, with the same characteristics, a valley in ρ_{xx} and a plateau in ρ_{xy}, was only observed at full fillings of Landau levels.

The plateau, which was observed forming at $v = \frac{1}{3}$ as shown in $Figure\ 5.1$, therefore could not have been the result of IQHE. The newly found phenomenon was later named fractional quantum Hall effect (FQHE) for occurring at fractional fillings of Landau levels and it's underlying physics is substantially different from the physics underlying the IQHE.

The Coulomb interaction in a two-dimensional electron system (2DES) subjected to a quantizing magnetic field leads to the formation of new, fractionally charged quasiparticles at Landau level filling factors $v = \frac{p}{q}$(q is an odd-integer)[14].

When our conductor is clean and electron-electron interaction is dominant with high mobility of electrons, we expect fractional quantum hall effect. Number of fractional values increases by higher mobility and lower temperature.

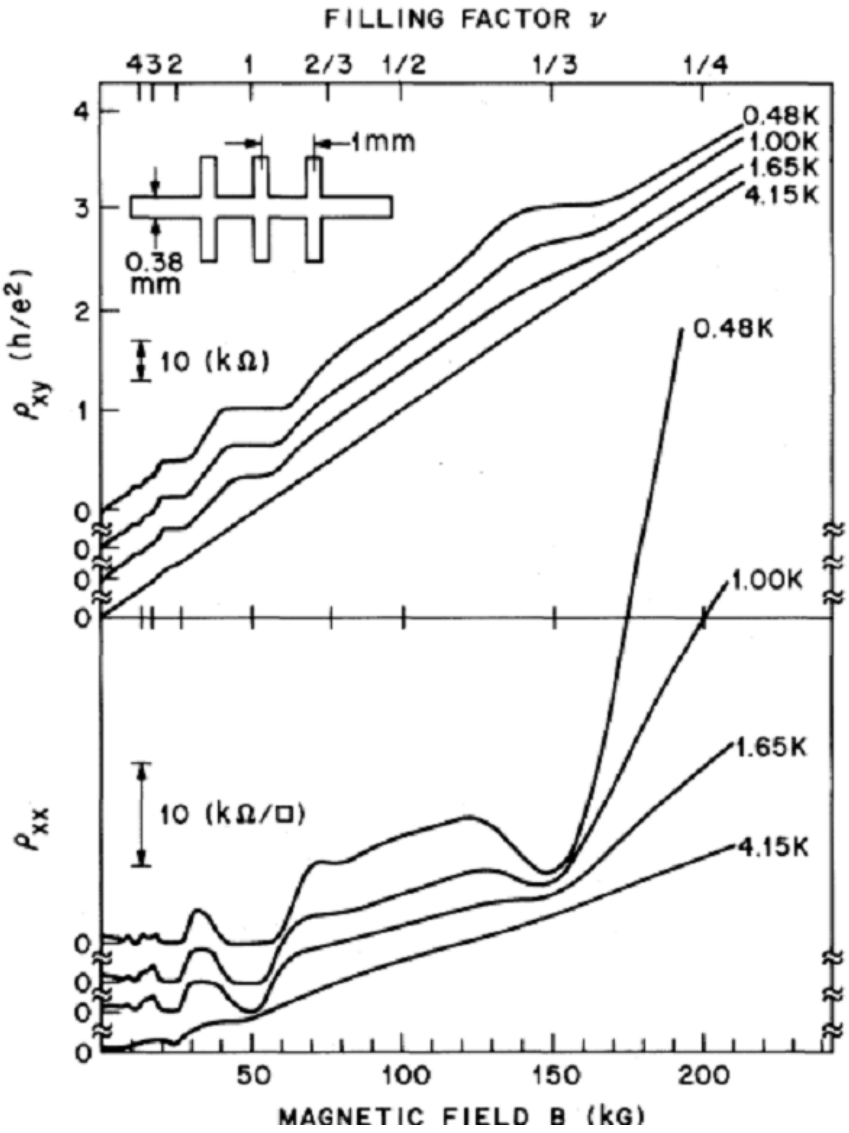

Figure 5.1: Measurements made by Tsui, Stormer, and Gossard, showing formation of a plateau in Hall resistivity ρ_{xy} at $\frac{1}{3}$ filling of the first Laundau level, with diagonal part of the resistivity tensor ρ_{xx}having a dip at the same filling factor. Sample geometry is shown in the top left corner.

More detail explanation of the Fractional quantum Hall effect will be provided in the following subtopic under Fractional quantum Hall effect.

5. 1 laughlin's trial wave function

In order to understand the problem of interaction in the lowest landau level, Laughlin proposed a trial wave function in 1983 based on a many body problem, as follow[15].

Symmetric gauge, working in two dimensional complex coordinates z = $x + iy$ the wave function of a N-electron system that is confide to the lowest landau level can always be written as the product of a function f analytic in all the electron coordinate z_1, z_2,… z_N with a gaussian factor.

Laughlin's main contribution to the FQHE was his trial wave function, shown schematically on $Figure$ 5.2, His prototype ground state[16]

$$\Psi(z_1,z_2,\ldots z_N) = f_N(z)\, e^{-\sum_{i=1}^{N} \frac{|z_i|^2}{4l_0^2}} \tag{5.1}$$

where from the pauli principle that f is totally antismmertic and $l_0 = \sqrt{\frac{\hbar}{e\boldsymbol{B}}}$ is the magnetic length and z = $x + iy$ is complex coordinates of two dimensional electron.

As the gaussian is factor set by the cyclotron degree of freedom, the Hiblert space of the lowest landau level reduce to the space of analytic function in N complex variables.

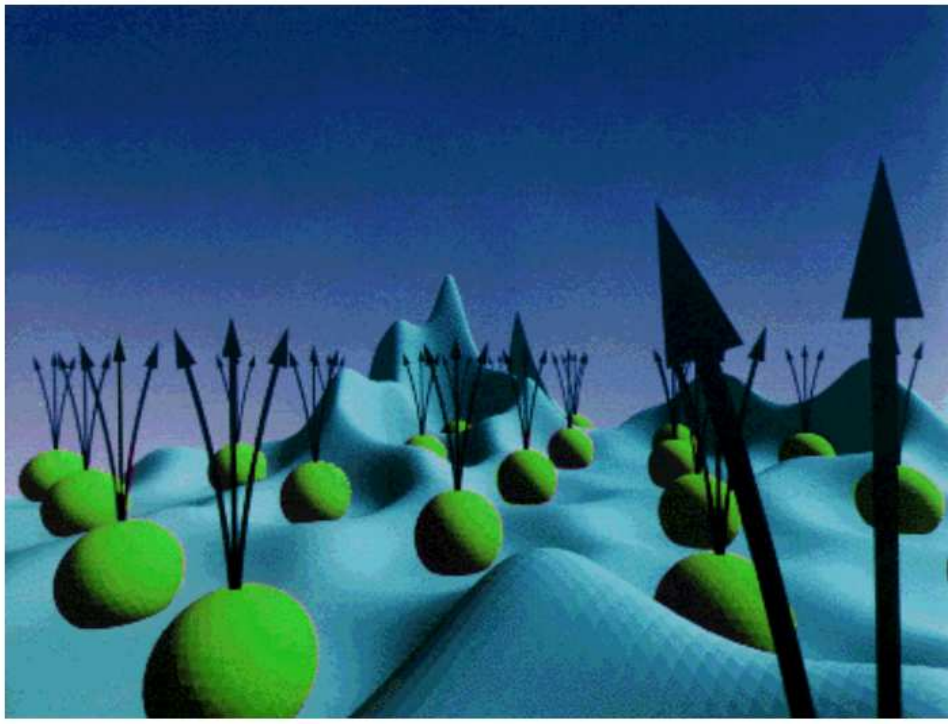

$Figure$ 5.2: Charge distribution of a prototype electron for the $v = \frac{1}{3}$ Laughlin wave function. The green spheres represent electrons, while the black arrows represent flux quanta.

An orthonormal basis of single-particle states for the lowest Landau level is thus provided by function of the form

$$\varphi_k(z) = \frac{z^k}{\sqrt{2\pi 2^k k!}} e^{\frac{-|z|^2}{4l_0^2}}. \qquad (5.2)$$

These states each have angular momentum k and it is easy to show that their probability density is peaked at radius $\sqrt{2k}$.

Laughlin made the following guess for the wave function at $\nu = \frac{1}{m}$, m odd[17]

$$f_N^m(z) = \prod_{i>j}^{N}(z_i - z_j)^m, \qquad (5.3)$$

Since m is an odd integer, analyticity and antisymmetry are immediate. In addition, the m = 1 state is simply a Slater determinant built out of the single-particle states φ_k, i.e.

$$\Psi_N^1(z) = \begin{vmatrix} \varphi_{0(z_1)} & \varphi_{0(z_2)} & \varphi_0(z_N) \\ \varphi_{1(z_1)} & \varphi_{1(z_2)} & \varphi_1(z_N) \\ . & . & . \\ . & . & . \\ . & . & . \\ \varphi_{N-1}(z_1) & \varphi_{N-1}(z_2) & \varphi_{N-1}(z_N) \end{vmatrix}, \qquad (5.4)$$

which clearly corresponds to a filled lowest Landau level. For m> 1, we verify that Ψ_N^m has the correct filling as follows. Since the highest degree of any of the $z_i s$ in f is m(N − 1), it follows that this is the highest possible angular momentum in the decomposition of Ψ_N^m in the single-particle basis. The area of the droplet described by Ψ_N^m is given by A = 2π$ml^2(N - 1)$; If the sample has area A, the maximum possible number quantum states of the system is

$$N_\Phi = \frac{A}{2\pi l^2}$$

$$= \frac{2\pi m l^2(\mathrm{N}-1)}{2\pi l^2}$$

$$= m(N - 1)$$

According to Jain, filling factor, is equal to the ratio of total number of electrons to the total number of flux quanta

$$\nu = \frac{N}{N_\Phi} = \frac{N}{m(N-1)} \quad \text{For N}\rightarrow\infty,$$

$$\nu = \lim_{\mathrm{N}\to\infty} \frac{N}{m(N-1)} = \frac{1}{m}, \qquad (5.5)$$

That corresponds to the Laughlin sequence of the FQHE (or called Laughlin state). Thus, we have produced a trial wave function that has the correct filling and lives entirely in the lowest landau level.

The Laughlin wave function has an additional and extremely useful property: we can show that it is the exact ground state for a short-range model Hamiltonian. The Hamiltonian has no kinetic part in the lowest landau level. It is given simply by the interaction V, which depend only on the relative motion.

To see this we observe, following Haldane, that we can expand any translationally and rotationally invariant two-body interaction projected onto a lowest Landau level as.

$$V = H = \sum_{m'}^{\infty} \sum_{i>j} V_{m'} p_{m'}(ij), \tag{5.6}$$

where $p_{m'}$(ij) are operators that project onto states such that particle i and j have relative angular momentum m. The coefficients of the expansion, $V_{m'}$ are known as Haldane pseudopotentials and depend on the Landau level under consideration; for repulsive interactions they are all positive. Since the projectors for different angular momenta do not commute, this rewriting does not immediately simplify the problem. However, if we consider a model Hamiltonian defined by $V_{m'} > 0$ for m'< m and zero otherwise, then it is clear that the Laughlin state Ψ_N^m[z] is an exact, zero-energy eigenstate for any N, since any two electrons have a relative angular momentum of at least m. It is also possible to show that the model Hamiltonian has a gap, since any excitation involves reducing the relative angular momentum of at least one pair of electrons and therefore costs positive energy.

5.2 Plasma Analogy

The Laughlin wavefunction exemplifies another extremely useful property in common with several different wave functions that share its Jastrow (pair product) form, namely that the ground state correlations reduce to the finite-temperature equilibrium correlations of an interacting classical system in the same dimension. This is accomplished by computing the ground state probability density and noting that it can be written as a classical Boltzmann weight[16]

$$||\Psi_N^m(z)||^2 = e^{-\beta H_{cl}}, \tag{5.7}$$

And choosing $\beta = \frac{1}{m}$, then one can obtain the energy of a 2D coulomb plasma of particle of charge –m.

$$H_{cl} = -2m^2 \sum_{i<j} \log|z_i - z_j| + \frac{m}{2l^2} \sum_k |z_k|^2, \tag{5.8}$$

The Hamiltonian model including coulomb interaction between electrons $V(r_j - r_k)$ and the ion potential $V_{ion}(r_j)$ is written as

$$H = \sum_j^N \{\frac{1}{2m}\{\hat{p}_j - \frac{e}{c}\boldsymbol{A}(r_j)\}^2 + V_{ion}(r_j)\} + \sum_{j<k}^N V(r_j - r_k), \quad (5.9)$$

By comparing Eq. (5.8) and Eq. (5.9), the first term in Eq. (5.8) can be described as coulomb repulsion of particle of charge m in two dimensions while the second one represents a uniform "charge" density $\frac{1}{2\pi l^2}$ being attracted to the origin. The particle need to have density $\rho = \frac{1}{2\pi m l^2}$, if local electric neutrality is to be present. It can be readily seen, why the proposed wave function could work well. Having an odd m the wave function is anti-symmetrical to the particle exchange, which is required due to electrons being fermions. Furthermore, such a state exhibits the preference of having the particle density of $\rho = \frac{1}{2\pi m l^2}$, which leads to the formation of the plateaus in transversal resistivity ρ_{xy}.

5.3 Fractionally Charged Excitations

The Quantum Hall States have charged quasiparticle excitations, conventionally referred to as quasielectrons and quasiholes, corresponding to negative and positive charge respectively. These are nucleated when the filling factor is altered from a commensurate value, either by varying the charge density or the magnetic field. The wavefunction for a quasihole located at Z is[17]

$$\Psi^m_{qh,N}(z, Z) = \prod_{i=1}^N (z_i - Z)\Psi^m_N(Z), \quad (5.10)$$

When translated into a physical electric charge, the quasihole represents an excitation with fractional electric charge, the fractional charge of e^* of the hole is given by[18]

$$e^* = \frac{-e}{m} \quad (5.11)$$

To obtain a quasielectron wavefunction we should simply replace the product in the quasihole wavefunction with its complexconjugate, but this leads to a wavefunction that is not restricted to the lowest Landau level. Projecting back to the restricted Hilbert space, the $z_i^* s$ are mapped to derivatives, leading to [17]

$$\Psi^m_{qe,N}(z, Z) = \prod_{i=1}^N (2\frac{\partial}{\partial z_i} - Z^*)\Psi^m_N(Z), \quad (5.12)$$

with effective charge $e^* = \frac{+e}{m}$ localized near Z (and an equal spread-out negative charge).

Where the derivatives act only on the polynomial part of Ψ_N^m . Owing to the rather complicated form of the quasielectron wavefunction, we shall work primarily with quasiholes in the following.

The quasihole wavefunction can also be studied using the plasma mapping, which leads to a classical Boltzmann weight of the form $e^{-\beta(H_{cl}+H_i)}$. Here H_{cl} and β have the same values as in $Section$ 5.2, and

$$H_i = -m\sum_{i=1}^{N}\log|z_i - Z|, \tag{5.13}$$

is the energy of unit charge impurity at Z interacting with the mobile charge-m particles of the plasma. Since the plasma attempts to maintain charge neutrality it will screen the impurity. The resulting screening cloud has a net deficit of $\frac{1}{m}$ plasma particles.

5.4 Composite-fermion approach

Trial wave function proposed by Laughlin only covers the filling factors of type $\frac{1}{m}$. Other theories emerged later, such as hierarchical scheme by Haldane and Halperin and composite fermions approach proposed by Jain, which try to provide an microscopic explanation for other observed states, not only for $\frac{1}{m}$ states. We have seen that the filling factor ν plays a very important role in QHE. It determines the behaviour of the 2DES, namely whether it manifests IQHE or FQHE.

Composite Fermions are quasi-particles constructed of interacting electrons confined to a plane and an even number of flux quanta attached to them. They have been introduced in order to explain the features in the high-magnetic field magneto- and Hall conductances in the region of the Fractional Quantum Hall Effect (FQHE)[19].

Laughlin and Arovas et al. observed the equivalence, in a mean field sense, of a uniform liquid of electrons in a magnetic field with the average flux per electron area of $m\Phi_0$ and of a uniform liquid of electrons, each carrying with it a flux of $m\Phi_0$[20]. As an analogy to type II superconductors, the magnetic field $\boldsymbol{B}$ piercing the electron gas can be viewed as forming of vortices or flux tubes within the liquid of electrons, one per flux quantum Φ_0, as shown as a part of $Figure$ 5.3. The electronic charge within the vortex is zero at its centre and average surrounding charge density at its edge. As such vortex is basically the same as the absence of electrons it is particularly beneficial to put a vortex on top of an electron due to Coulomb repulsion. If enough vortices are present, placing more of them onto the electron further reduces the repulsive energy.

Putting a vortex onto an electron is the same as the attachment of a flux quantum, generating the vortex, to the charge carrier thus creating new entities called composite particles (CP).

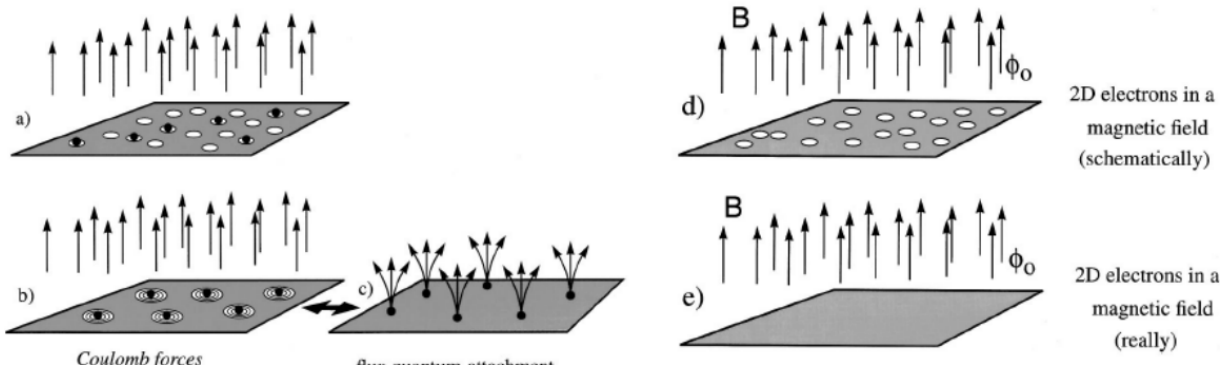

Figure 5.3: Schematic drawing of electron vortex attraction at Landau-level filling $\nu = \frac{1}{3}$. a) The Pauli principle is satisfied by placing one vortex onto each electron. b) Placing more vortices onto each electron further reduces Coulomb repulsion. c) Vortex attachment can be viewed as the attachment of magnetic flux quanta to the electrons, creating composite particles. d) and e) show the 2DES in a magnetic field described with vortices.

Electrons are fermions and generate a -1 phase shift with the exchange of the position of two electrons. Exchange of each flux quantum $\Phi_0 = \frac{hc}{e}$ multiplies the wave function by an additional -1. The statistics of CP therefore depend on, as Jain proposed, the number of flux quanta per charge carrier. If the magnetic field generates an even number of flux quanta per charge the resulting CP obey the Fermi-Dirac statistics, hence can be called composite fermions (CFs), while an odd number of flux quanta per charge gives rise to composite bosons (CB). The main idea of this approach is that, since the relevant correlations between CFs are the correlations due to their Fermi statistics, the FQHE for electrons is a manifestation of the IQHE for CFs.

Since a vertox ≈ a flux quantum, it is intuitively useful to view composite fermions as;

CF = electrons + $2m$ flux quanta.

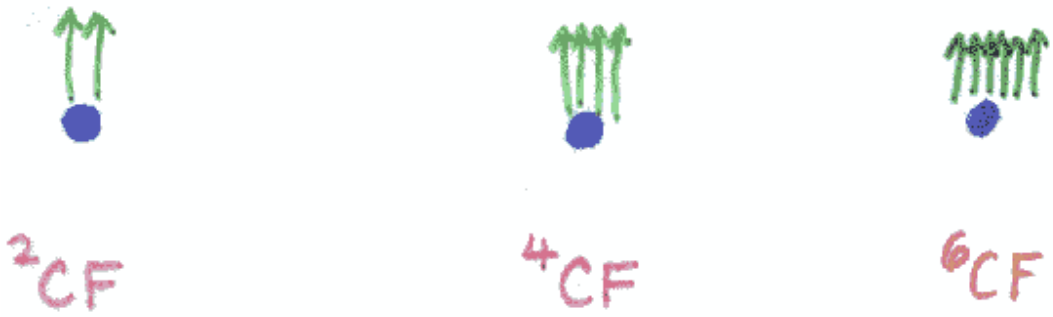

The leftover vortices, which haven't been used for formation of CF, represent an effective field B* of[21]

$$\boldsymbol{B}^* = \boldsymbol{B} - 2mn\Phi_0, \tag{5.14}$$

where n denotes two-dimensional carrier density. Composite fermions form Landau-like levels in $\boldsymbol{B}^*$ with the filling factor

$$\nu^* = \frac{nhc}{e\boldsymbol{B}^*}, \tag{5.15}$$

In analogy with electrons for integer ν^* of IQHE for CF manifests, thus producing plateaus in Hall resistivity when filling factor for electrons ν satisfies the demand

$$\nu = \frac{\nu^*\boldsymbol{B}^*}{\boldsymbol{B}} = \frac{\nu^*}{2\mathrm{m}\nu^* \pm 1}, \tag{5.16}$$

where ± 1 once again denotes the direction of $\boldsymbol{B}^*$compared to $\boldsymbol{B}$.

For m = 1 (compensation of the external magnetic field at half filling) one obtains for ν^* = 1, 2, 3 . . . the sequences (= $\frac{1}{3}, \frac{2}{5}, \frac{3}{7}$, . . . and for ν^*= -1, -2, -3, . . . the sequences (= 1, $\frac{2}{3}, \frac{3}{5}$, . . . which are consistent with the filling factors at which the FQHE is observed.

5.5 Hierarchies

The original Laughlin formalism only described states occurring at $\nu = \frac{1}{3}$ fractional filling of the lowest LL; however, it experiments show a host of other fractions which are not simple Laughlin fillings. After the first discovery of the $\nu = \frac{1}{3}$ fractional state, however, the FQHE was observed at many fractional fillings throughout the first and second Landau levels, occurring in general at $\nu = \frac{p}{q}$ where q is an odd integer and p being an integer[22]. Such factors arise when the density of quasiparticles becomes too high and consequently the quasiparticles delocalize and condense into a Laughlin state of their own. Such phenomenon is known as hierarchy.

Haldane and Halperin extended the work of Laughlin to explain these other fractional states by introducing the hierarchical model. In the standard hierarchical model, the Laughlin states ($\nu = \frac{1}{3}$) are identified as "primary" fractions. Other fractions are then interpreted as "daughter states", resulting from a Laughlin-like condensation of quasi-particles formed from the parent states of the primary fractions.

How are we to understand these new fractions? The solution lies in any of a number of 'hierarchy constructions' that in effect reduce the problem non-Laughlin fillings to an already

solved problem. One approach – pioneered by Haldane and Halperin – is to arrange affairs so that the quasiparticles of an existing quantum Hall state themselves form a Laughlin liquid. Another idea, due to Jain, is to consider the fractional quantum Hall effect as the integer effect of a new 'composite' fermion.

We start with the Haldane-Halperin hierarchy construction, which proceeds iteratively at as follows: fractional Quantum Hall States at a given level of the hierarchy are obtained by forming Laughlin states of the quasielectrons or quasiholes of the previous level; the uppermost level of the hierarchy consists of the Laughlin states. One begins by inserting quasiparticles into a Laughlin state of electrons called state L_1. The quasiparticles then correlate together to form a Laughlin state of their own, called state L_2. Now, it is absolutely possible to introduce a further set of quasiparticles in the state L_2 such that these new quasiparticles yield a further Laughlin state L_3.

Let us begin with a parent Laughlin state with $\nu = \frac{1}{3}$, and discuss how to construct the next level of the hierarchy. As we have shown previously, $in\ section\ 5.1$, and filling factor at commensuration are related by $N_\Phi = m(N - 1)$. If we in addition add N_{qp} quasiparticles, this is replaced by

$$N_\Phi = m(N - 1) + \alpha N_{qp}\ , \tag{5.17}$$

with $\alpha = -1(+1)$ for quasielectrons (quasiholes). If we now require that the added quasiparticles are themselves in a Laughlin $\frac{1}{m}$ state, we must have a similar condition

$$N = p(N_{qp} - 1), \tag{5.18}$$

with p even. The evenness of p is because the quasiparticles are nominally bosonic, and so they can only form even denominator Laughlin states. The replacement of N_Φ by N is because the number of independent single-quasiparticle states is N rather than N_Φ, which is the number of available electronic states. From Eq. (5.17) and Eq. (5.18), it follows that in the thermodynamic limit the first-level hierarchy state has filling

$$\nu = \frac{N}{N_\Phi} = \frac{p}{mp + \alpha'}, \tag{5.19}$$

To determine the charge carried by quasiparticle of the hierarchy state, consider adding a single electron to the system, so that we take $N \rightarrow N^0 + 1$. We then have

$$N_\Phi = m(N^0 + 1 - 1) + \alpha N_{qp}^0$$

$$= m(N^0 - 1) + \alpha(N_{qp}^0 + \alpha m)$$

$$\equiv m(N^0 - 1) + \alpha N_{qp}, \tag{5.20}$$

where we have defined a modified quasiparticle number $N_{qp} = N_{qp}^0 + \alpha m$, which follows from the fact that an electron is equivalent to αm Laughlin quasiparticles. We then find

$$\begin{aligned} N^0 + 1 &= p(N_{qp}^0 - 1) + 1 \\ &= p(N_{qp}^0 + \alpha m - 1) - \alpha(mp - \alpha) \\ &= p(N_{qp} - 1) - \alpha(mp - \alpha), \end{aligned} \tag{5.21}$$

which corresponds to a state with $(mp - \alpha)$ quasiparticle excitations of the daughter incompressible fluid. It follows that the latter have charge $\frac{\pm 1}{mp-\alpha}$ i.e. the reciprocal of the denominator of the filling fraction.

By iterating this procedure, one can construct an infinite hierarchy of incompressible states, at filling factors given by appropriately terminating the continued fraction[23]

$$\nu = \cfrac{1}{m + \cfrac{\alpha_1}{p_1 - \cfrac{\alpha_2}{p_2 - \cdots}}}, \tag{5.22}$$

Where $\alpha_i = \pm 1$ or 0 (it becomes 0 when quasiparticles are no longer introduced) and p_i is a even positive integer. The hierarchy table for $q = 3$ is shown on $Fig.5.4$. At every level of the hierarchy, the pseudopotentials acting between the quasiparticles must be short-range enough in order for the Laughlin state to emerge.

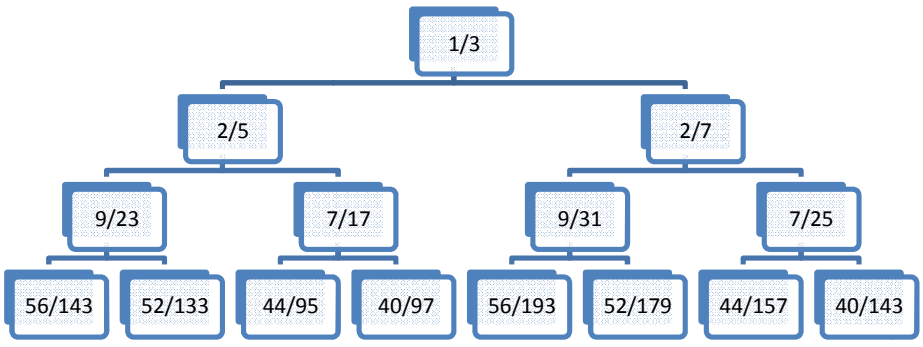

$Figure$ 5.4: Hierarchy table for $m = 3$.

5.6 The fractional quantum hall effect in graphene

5.6.1 Introduction to graphene

Graphene is a single 2D layer of carbon, packed in a heksagonal (honeycomb) lattice, with a carbon distance of 0.142 nm[24, 25]. Graphene alternatively defined as, One-atom-thick 2D electron gas in which electrons behave as massless relativistic charged fermions.

5.6.1.1 Crystal structure of graphene

As mentioned, graphene is a 2D crystal with hexagonal structure consisting of a bipartite lattice of two triangular sublattices (because each unit cell contains two carbon atoms) as shown in fi$gure$ 5.5. There are two C atoms per unit cells. The crystal structure can be represented by two basis vectors a_1 and a_2 in the plane xOy, and has a triangular Bravais lattice. There are two carbon atoms in each unit cell, which we denote by A (red dots) and B (the blue dots) in $Fig.5.5$. We choose atoms A as our triangular lattice whose basis vectors are[25]

$$a_1 = a\left(\frac{1}{2}, \frac{-\sqrt{3}}{2}\right), \tag{5.23a}$$

$$a_2 = a(1, 0), \tag{5.23b}$$

where a = $3\sqrt{c}$; c = 1:42$\dot{A}$, and c is the distance between two nearest neighbor atoms.

We can move one red atom $(A\ atom)$ to any point in the A-sublattice by the translation vector $R = n_1a_1 + n_2a_2$. Hence, the reciprocal lattice vectors are given by

$$b_1 = \frac{2\pi}{a}\left(0, -\frac{2}{\sqrt{3}}\right), \tag{5.24a}$$

$$b_2 = \frac{2\pi}{a}\left(1, \frac{1}{\sqrt{3}}\right), \tag{5.24b}$$

which is also a regular hexagonal lattice as shown in $Fig.5.6$.

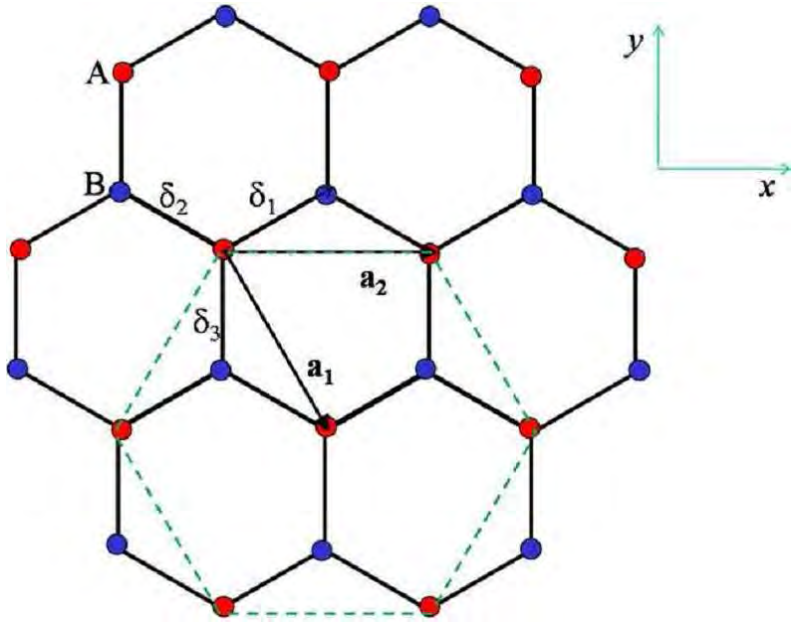

Figure 5.5: Graphene crystal lattice. Each red atom is linked to its three nearest neighbors by vectors δ_1; δ_2; δ_3. The C atoms can be separated into two kinds of atoms denoted by red (A) and blue (B) dots, i.e. we can divide the whole lattice into two sublattice whose lattice vectors are a_1 and a_2.

Each atom is tied to its three nearest neighbors via strong δ bonds that lie in the graphene plane with angles of 120°. The forth valence electron is in the $2p_z$ orbital that is orthogonal to the graphene plane. The three nearest blue neighbor atoms of one red dot are separated by

$$\delta_1 = a\left(\frac{1}{2}, \frac{1}{2\sqrt{3}}\right), \tag{5.25a}$$

$$\delta_2 = a\left(-\frac{1}{2}, \frac{1}{2\sqrt{3}}\right), \tag{5.25b}$$

$$\delta_3 = a\left(0, -\frac{1}{\sqrt{3}}\right), \tag{5.25c}$$

as shown in *Fig*. 5.5.

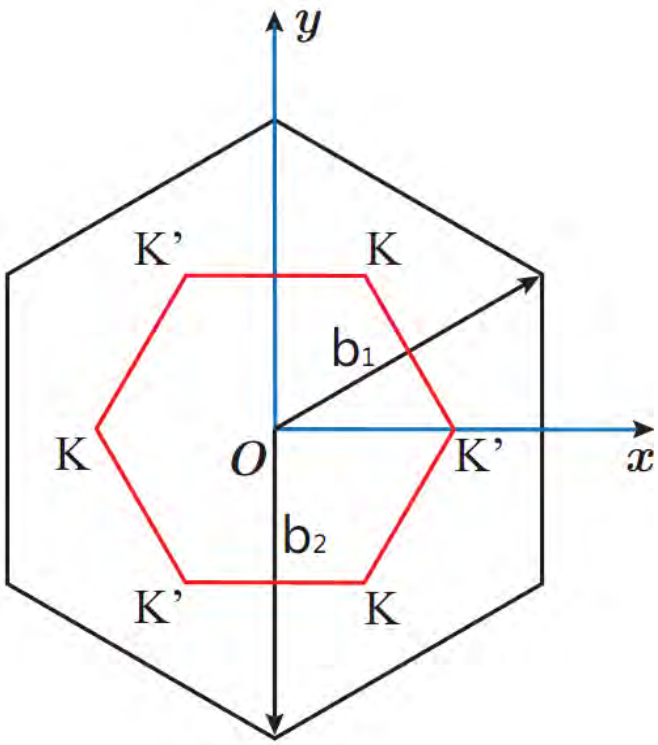

Figure 5.6: Reciprocal lattice based on $\{b_1; b_2\}$ and the first Brillouin zone represented by the red regular hexagon.

The first Brillouin zone that is the smaller regular hexagon plotted in *Fig.* 5.6. In the first Brillouin zone, there are two inequivalent points respectively, K and K'. Each K or K' point can be translated to other equivalent K or K' by a combination of the two basis vectors of the reciprocal lattice. We choose

$$K = \frac{2\pi}{a}(-\frac{2}{3}, 0), \tag{5.26a}$$

$$K' = \frac{2\pi}{a}(\frac{2}{3}, 0), \tag{5.26b}$$

5.6.2 Landau level in graphene

Landau quantization in quantum mechanics is the quantization of the orbits of charged particles in magnetic fields as a result; the charged particles can only occupy orbits with discrete energy values, called Landau level.

Let us come now to the case of graphene. Actually we would naively expect graphene to be an example case for two dimensional electron gases due to its perfect two dimensional crystal structure. Thus we expect landau level in graphene.

We start by considering the classical Dirac Hamiltonian. According to theory of Relativity we can get two type dispersion relation of energy.

A stationary particle (p=0) (Non relativistic) has rest energy

$$E = mc^2, \tag{5.27}$$

And for a particle in motion is described by the relativistic dispersion relation

$$E = \sqrt{(mc^2)^2 + c^2p^2}, \tag{5.27}$$

From wave equation that given as $\Psi = e^{i(k.r-wt)}$ we have

$$E = \hbar\omega \sim i\hbar\frac{\partial}{\partial t};\ \vec{p} = \hbar k \sim -i\hbar\vec{\nabla}, \tag{5.28}$$

For relativistic particles energy is given by $E^2=c^2p^2 + m^2c^4$, then Schrodinger Equation will be written as follow

$$(-\hbar^2c^2\nabla^2+m^2c^4)\Psi = -\hbar^2\frac{\partial^2\Psi}{\partial t^2}, \tag{5.29}$$

Thus we have Hamiltonian

$$H = \vec{\alpha}c\vec{p} + \beta mc^2, \tag{5.30}$$

where the Hermitian, dimensionless matrices $\vec{\alpha}$ and β are to be determined and $\vec{p}$ denote the three-dimensional momentum vector. The requirements to α, β are next

$$\beta^2 = 1,\ \ \beta\alpha_i + \beta\alpha_j = 0\ \ \alpha^2 = 1, \tag{5.31a}$$

$$\alpha_j\alpha_i + \alpha_i\alpha_j = 2\delta_{ij}(i = x, y, z), \tag{5.31b}$$

In the two dimensional case the Dirac matrices can be identified with the Pauli matrices:

$\alpha_1 = \sigma_x;\ \alpha_2 = \sigma_y\ \ \beta = \sigma_z$, then for massless fermions Dirac Hamiltonian is

$$H = \boldsymbol{V}_F\,\vec{\sigma}.\hat{p} \quad \text{..... (5.32)}$$

Where $\vec{\sigma} = (\sigma_x, \sigma_y)$, $\boldsymbol{V}_F$ is Fermi velocity, velocity of electron in the graphene, and $\hat{p}$ is momentum operator.

Let's show that Dirac Hamiltonian shows the same results for massless particle Putting (5.30) in square and applying properties of Pauli matrices that defied in $Eq.5.31$ a and b, one obtains

$H^2 = m^2c^4 + c^2\vec{p}^2$, then $\ E_{\vec{p}} = \sqrt{m^2c^4 + c^2\vec{p}^2}$

for massless particle m =0 and if to count from the Fermi level $c \rightarrow \boldsymbol{V}_F$. The Fermi velocity $\boldsymbol{V}_F$ is $\sim \frac{1}{300}$ the speed of light c. We have slow ultrarelativistic electrons[26]

$$E_{\vec{p}} = \boldsymbol{V}_F |\vec{p}|, \tag{5.33}$$

All massless particles have the same energy dispersion as photons. Therefore quasiparticles in graphene are massless particles described by the equation (5.33) or (5.32).

Now we consider the problem of a uniform magnetic field $\boldsymbol{B}$ applied perpendicular to the graphene plane. Here we use a simple method in first quantized language to give the solutions to the problem. In the presence of a magnetic field, $-i\hbar\nabla$ in Eq. (5.32) should be replaced by $-i\hbar\nabla + \frac{e\boldsymbol{A}}{c}$ [27], thus the Schrodinger Equation be come

$$\boldsymbol{v}_f[\vec{\delta}.(-i\hbar\nabla + \tfrac{e\boldsymbol{A}}{c})]\Psi(r) = E\Psi(r) \tag{5.34}$$

If we take the Landau gauge: $\boldsymbol{A} = \boldsymbol{B}(-y, 0)$ and write the wave function as the form of $\Psi(x,y) = e^{ikx}\phi(y)$, then the Dirac equation will read

$$\hbar\boldsymbol{v}_f \begin{pmatrix} 0 & \partial_y - k + \frac{e\boldsymbol{B}y}{\hbar c} \\ -\partial_y - k + \frac{e\boldsymbol{B}y}{\hbar c} & 0 \end{pmatrix} \phi(y) = E\phi(y) \tag{5.35}$$

afrer defining, $l_{\boldsymbol{B}} = \sqrt{\frac{\hbar C}{e\boldsymbol{B}}}$, $\omega_c = \frac{\sqrt{2}\boldsymbol{v}_f}{l_{\boldsymbol{B}}}$, $\xi = \frac{y}{l_{\boldsymbol{B}}} - l_{\boldsymbol{B}}k$, $\hat{a} = \frac{1}{\sqrt{2}}(\partial_\xi + \xi)$, $\hat{a}^+ = \frac{1}{\sqrt{2}}(-\partial_\xi + \xi)$ then $Eq.(5.35)$ becomes

$$\hbar\omega_c \begin{pmatrix} 0 & \hat{a} \\ \hat{a}^+ & 0 \end{pmatrix} \phi(\xi) = E\phi(\xi), \tag{5.36}$$

Since the canonical communication relation: $[\hat{a}, \hat{a}^+] = 1$ is satisfied, the eigenvectors can be constructed from the eigenfunctions of a harmonic oscillator, ϕ_n. The obtained eigenvectors and energy eigenvalues are given by

$$\phi_{n,\pm}(\xi) = \begin{pmatrix} \varphi_{n-1}(\xi) \\ \pm\varphi_n(\xi) \end{pmatrix}, \tag{5.37}$$

Thus $\hbar\omega_c\hat{a} \pm \varphi_n(\xi) = E_n\,\varphi_{n-1}(\xi)$ and $\hbar\omega_c\hat{a}^+\varphi_{n-1}(\xi) = E_n \pm \varphi_n(\xi)$ which yields the equation; $\hat{a}^+\hat{a} \pm \varphi_n(\xi) = (\frac{E_n}{\hbar w_c})^2 \pm \varphi_n(\xi)$

$$E_n = \pm\hbar\omega_c\sqrt{n} = \pm\sqrt{\frac{2\hbar eBn}{c}}, \tag{5.38}$$

Where n =0,1,2,3,…

These discrete energy eigen value are the ladau level in the graphene.

In graphene the Landau levels are four fold degenerate due to the two nonequivalent valleys and the two possible spin directions.

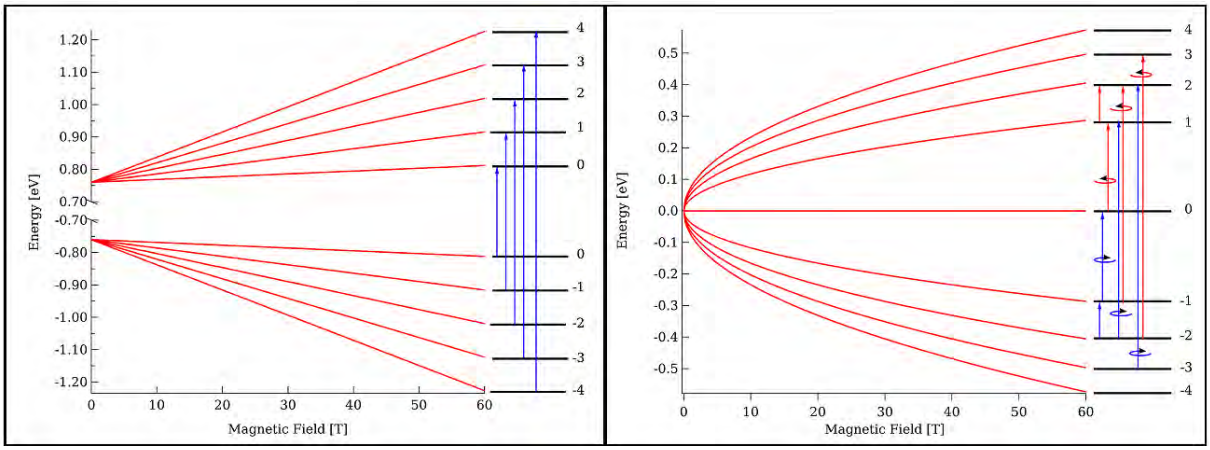

Figure 5.7 – (a) Linear Landau level bands for GaAs quantum well with an effective mass of $m* = 0.067\ .m_e$. Note the electron ($E > 0$) and hole ($E < 0$) bands are separated by an energy gap of approximately 1.5 eV. We include optical inter-band transitions. (b) Landau levels in graphene are following the $\sqrt{B}$ dependence. On the right hand side of the figures the selection rules for Landau level transitions are sketched. The blue and red arrows should have the same strength. We can distinguish both transitions using circularly polarised light.

We are now able to make some remarks and pick out some differences in comparison to the conventional case of two dimensional electron gases. The first obvious and most important difference is the $\sqrt{Bn}$ dependence of the Landau levels in graphene. It is the signature of relativistic and massless particles. Another point which differs from the usual case is the fundamental Landau level (n = 0). In graphene the energy of this level is

$$E(\mathbf{B}, 0) = 0, \tag{5.39}$$

which is in contrast to our findings for two dimensional electron systems with parabolic dispersion where we obtain for the fundamental Landau level ($n = 0$)

$$E(\boldsymbol{B}, 0) = \frac{\hbar w}{2}, \tag{5.40}$$

The E = 0 state remains an intriguing case. It is a level shared by electrons and holes simultaneously in the absence of doping.

5.6.3 Observation of fractional quantum hall effect in graphene.

When electrons are confined in two dimensions and subject to strong magnetic fields, the Coulomb interactions between them can become very strong, leading to the formation of correlated states of matter, such as the fractional quantum Hall liquid. In this strong quantum regime, electrons and magnetic flux quanta bind to form complex composite quasiparticles with fractional electronic charge; these are manifest in transport measurements of the Hall conductivity as rational fractions of the elementary conductance quantum. The experimental discovery of an anomalous integer quantum Hall effect in graphene has enabled the study of a correlated two-dimensional electronic system, in which the interacting electrons behave like massless chiral fermions. However, owing to the prevailing disorder, graphene has so far exhibited only weak signatures of correlated electron phenomena, despite intense experimental and theoretical efforts[28].

When charge carriers such as electrons are confined to moving in a two-dimensional plane and subject to a perpendicular magnetic field, they can form new quasi-particles with a fraction of the electron's elementary charge. This is known as the fractional quantum Hall effect FQHE. Graphene could be considered such a perfect two-dimensional system because the carbon atomic constituents are arranged in a single plane. Its charge carriers are remarkably mobile and have been predicted to interact strongly with each other. Thus we expect FQHE in graphene.

The FQHE in graphene is expected to deviate in important ways from that in GaAs-based 2DESs. First, electrons in graphene are considerably more two dimensional than in GaAs quantum wells, where the well widths range from 10 to 30 nm. This makes the interaction at short distances in graphene much stronger than in quantum wells. The interactions in SG are further enhanced owing to the absence of substrate screening ($\varepsilon \sim 1$) in contrast to GaAs where $\varepsilon \sim 13$. Stronger interaction leads to a larger energy gap, and thus higher temperatures at which the FQHE can be observed. Another difference arises from the fourfold spin and valley degeneracy. Because of this degeneracy, the situation in graphene is more similar to that realized in double quantum wells rather than in single quantum-well systems. However, electron interactions in graphene correspond to nearly identical intra- and inter-well interactions, a regime nearly impossible to achieve in GaAs systems. This leads to an SU(4) symmetry of the interaction Hamiltonian, and the prediction of new FQHE states with no analogue in GaAs.

The FQHE has not yet been conclusively observed experimentally in graphene but it has been explored theoretically in a number of papers.

5.6.4 The quantized Hall conductivity of the fractional quantum hall effect in graphene

In high magnetic field, each electron captures an even number $2m$ of quantized vertices to become a composite fermions are describe by an effective magnetic field by

$$\boldsymbol{B}^* = \boldsymbol{B} - 2mn\Phi_0, \tag{5.41}$$

Where n denotes 2D carrier density in the graphene. Composite fermions form Landau-like levels in **B*** with the filling factor $v* = \frac{nhc}{e\boldsymbol{B}^*}$ In analogy with electrons for integer v* of IQHE for CF manifests, thus producing plateaus in Hall resistivity when filling factor for electrons v satisfies the demand

$$v = \frac{v^*\boldsymbol{B}^*}{\boldsymbol{B}} = \frac{v^*}{2mv^*+1}, \tag{5.42}$$

the IQHE in graphene, the quantized Hall conductivity is found to be[24]

$$\sigma_{xy} = \pm 2(2n+1)\frac{e^2}{h} = \pm 4(n+\tfrac{1}{2})\frac{e^2}{h}, \tag{5.43}$$

where n is an integer here, the factor 2 is due to the spin degeneracy. In the case of graphene the effective filling factor v* is associated with the integer quantum Hall effect of composite particle and if we ignore the spin, then we can get v* from Eq. 5.43

$$v^* = 2n+1, \tag{5.44}$$

where n = 0,1,2……

hence, by combining Eq. 5.42 and 5.44, the quantized Hall conductivity in graphene in FQHE can by written as

$$\sigma_{xy} = \pm \frac{2n+1}{2m(2n+1)+1}\frac{e^2}{h}, \tag{5.45}$$

where the negative energy states corresponds to the Dirac hole or the valance band states in the graphene.

The quantized Hall conductivity of FQHE in graphene has been calculated. We have used the standard value of $\frac{e^2}{h}$ =2513Ω. Hence $\frac{e^2}{h}$ =3.874x10^{-5} Ω^{-1} we use $n \geq 0$ and m<0. The corresponding values of filling factors (v) are found to be; $\pm\frac{2}{3}, \pm\frac{2}{5}, \pm\frac{2}{7}, \pm\frac{6}{7}, \pm\frac{6}{13}, \pm\frac{6}{19}$,…….

Thus the FQHE in graphene has a sequence of states which is different from the sequence found in the 2D electron gas. Experimentally different filling factor are achieved by varing the applied magnetic field at a fixed electronic concentration.

The variation of σ_{xy} with respect to different values of filling factors is shown in Fig.

The unusual electronic dispersion of graphene is reflected in the varation of Hall conductance staircase. due to the special lattice structure of graphene and Dirac nature of carriers,

n	m	$v = \pm\frac{2(2n+1)}{2m(2n+1)+1}$	$\sigma_{xy} = v\frac{e^2}{h}$
0	1	2/3 = 0.6666	0.0000258
0	2	2/5 = 0.40	0.0000155
0	3	2/7 = 0.2857	0.0000110
1	1	6/7 = 0.8571	0.0000332
1	2	6/13 =0.4615	0.0000179
1	3	6/19 = 0.3157	0.0000122
2	1	10/11 =0.9090	0.0000352
2	2	10/21 = 0.4761	0.0000185
2	3	10/31 = 0.3225	0.0000125
3	1	14/15 = 0.9333	0.0000362
3	2	14/29 = 0.4827	0.0000187
3	3	14/43 = 0.3255	0.0000126

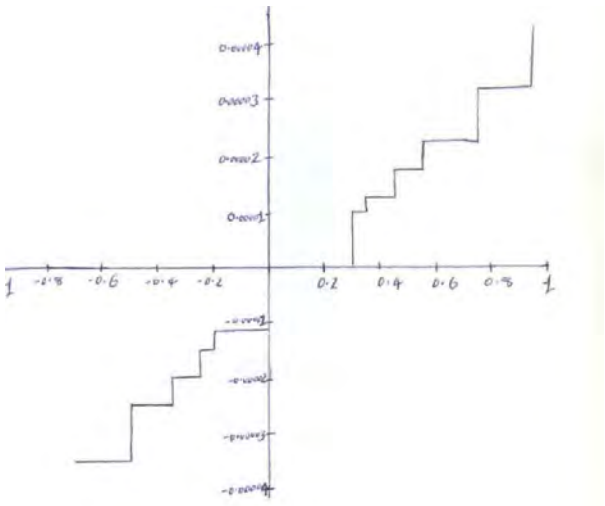

$Figure$. 5.8 Quantized Hall conductivity of graphene in fractional quantum Hall effect for different filling factors.

the edge state play a key role in quantum Hall transport. the edge state of v = 0 quantum Hall state carry no charge current but finite spine current in equilibrium.

CONCLUSION

Review of the present theoretical understanding of quantum Hall effect occurring in $2D$ electron gas with a strong B perpendicular to the system plane. The essential signatures are: resistivity component $\rho_{xx} \rightarrow 0$ as T → 0, with conductivity component $\sigma_{xy} = \frac{ve^2}{h}$ over a finite range of B ("Hall plateau"), where v is an integer or ratio of integers having odd denominator. Defining Landau filling factor as $v = \frac{nhc}{eB}$, where n is density of carriers. The integral effect is described by the interaction between electrons and impurities, while the fractional effect due to electron-electron correlations. To show quantized conductivity of quantum hall effect($i.e$ $\sigma_{xy} = \frac{ve^2}{h}$), we use two Arguments (Laughlin's Gendanken-Experiment and B$\ddot{u}$ttiker's Theory of Edge Currents).

Incompressible quantum fluid states arise when the filling factor is a rational fraction with odd denominator, because of restriction imposed on electron-electron correlations by the constraint that the electrons share the lowest landau level. we considered: laughlin's trial wave function, Composite-fermion approach and Hierarchies models proposed in literature in order to describe the filling factor of the fractional quantum hall effect. The laughlin's trial wave function shows some properties like; a short-range model Hamiltonian that described only by interaction V and given as, $V = H = \sum_{m'}^{\infty} \sum_{i>j} V_{m'} p_{m'}(ij)$, and in common with several different wave functions that share its Jastrow (pair product) form and this is accomplished by computing the ground state probability density. Which is given as $||\Psi_N^m(z)||^2 = e^{-\beta H_{cl}}$.

Graphene two dimensional carbon. Sheet of carbon atoms each with 3 covalently bonded nearest neighbors Graphene is two dimension of flat plateau of carbon because of this two dimension, in Graphene we expect theoretical fractional quantum hall effect.

Future outlook:

There are important research areas of Fractional Quantum Hall Physics which I have not considered (included) in this project. Even denominator filling factor, chern-simon mean-field theory of fractional quantum hall effect, The Spin Hall Effect in multilayer 2DES, Magnetoroton and Magnetoplasmon excitations in FQHE are some to mention. The study of Optoelectronic properties in Fractional Quantum Hall state, and High temperature Quantum Hall state are currently major research areas in Condensed Matter and Material Physics. My future prospective is to study these quantum phenomena.

Bibliography

[1]Raymond Vozzo(2005), Noncommutative Geometry and the Quantum Hall Effect (Thesis submitted for the degree of Honours in Pure Mathematics, the university of adeliade, Australia)

[2] Yohannis Ashenafi (2009), Quantized Hall Effect (Thesis submitted to Addis Ababa University).

[3] Olaf Smits(2008), Clustered states in the fractional quantum Hall effect, Master Thesis, Universiteit van Amsterdam

[4] Kittel, C. (2005) Introduction to Solid State Physics(8th.ed.). New York : John Wiley

& Sons, Inc.

[5] Klaus von Klitzing. (1985) The quantized hall effect. Nobel lecture.

[6] Y. AHARONOV AND D. BOHIN(1959) Significance of Electromagnetic Potentials in the Quantum Theory University.phy.lett.**115**, 3.

[7] Klitzing, v. K., (2005) Twenty five Years of Quantum Hall effect. Seminare.

[8] KAROL I. WYSOKIŃSKI() QUANTUM HALL EFFECT: THE FUNDAMENTALS: M. Curie-Sklodowska University Institute of Physics 20-031 Lublin, Poland

[9] Chetan Nayak (2004) Quantum Condensed Matter Physics – Lecture Notes

[10] Henrik Johannesson and Jari Kinaret(2007),Quantum Matter: Coherence And Correlations

[11] Dan Bohr, Christian Flindt, Thomas Frederiksen, Anders Mathias Lunde Copenhagen, (June 28, 2005) Topics in Quantum Transport Theory

[12] Ardavan Alamir(2008), Effects of Disorder and Interactions in the Quantum Hall Ferromagnet, Master Thesis, Utrecht University - Department of Physics and Astronomy

[13] Horst L. Stormer, Daniel C. Tsui and Arthur C. Gossard : The fractional quantum Hall effect

[14] H.L. Stormer, Two-dimensional electron correlation in high magnetic fields; Physica B 177 (1992) 401-408

[15] Zeleke Deressa Gerbi (2010) Field Theoretical Approach to Fractional Quantum Hall Effect (Thesis submitted to Addis Ababa University).

[16]Prasanta K. Panigrahi and M. Sivakumar(1995) Laughlin wave function and one-dimensional free fermions. Phys. Rev. B **52,** 19

[17] Pascal LEDERER, Introduction to the Quantum Hall Effects, Lecture notes, 2006

[18] A.J.Leggett, Laughlin wave function, Lecture 18 The FQHE:

[19] $B.Kramer^{1}$, $N.Magnoli^{2b}$, $E.Mariani^{1}$, $M.Merlo^{2a}$, $F.Napoli^{2a}$ and $M.Sassetti^{2a}$, Composite Fermions with Spin at v = 1/2.([1]I. Institut $f\ddot{u}r$ Theoretische Physik, Universit$\ddot{a}t$ Hamburg, Jungiusstraße 9

20355 Hamburg, Germany

[2a]INFM-Lamia, [2b]INFN, Dipartimento di Fisica, Universit$\grave{a}$di Genova, Via Dodecaneso 33

16146 Genova, Italy)

[20]J.K. Jain(1989) Composite-Fermion Approach for the Fractional Quantum Hall Effect.physrevlett.**63,**2

[21] J.K. Jain[a], R.K. Kamilla[b], K. Park[a], V.W. Scarola[a,]*, Interacting composite fermions, Solid State Communications 117 (2001) 117-122

[22]J. K. Jain(1989) Theory of the fractional quantum Hall effect. Phys.rev.B. **41**, 11

[23] Dingping Li(1992) Hierarchical Wave Functions of Fractional Quantum Hall Effect on the Torus, SISSA/ISAS/2/92/EP, cond-mat/9212034 January, 1992

[24] S.sahoo, india J pure and Appl. Phys, 49 (2011)

[25]Wenchen Luo(2009) Skyrmions in monolayer and bilayer graphene (Thesis submitted to UNIVERSIT$\acute{E}$ DE SHERBROOKE, Canada)

[26] BALÁZS DÓRA AND PETER THALMEIER, Magnetotransport and thermoelectricity in Landau-quantized disordered graphene, PHYSICAL REVIEW B **76**, 035402 (2007)

[27] Zuanyi Li (2008) Unconventional Quantum Hall Effect in Graphene,
PHYS 569: ESM term essay

[28] Kirill I. Bolotin1, Fereshte Ghahari, Michael D. Shulman, Horst L. Stormer & Philip Kim(2009) Observation of the fractional quantum Hall effect in graphene, letter nature volume **462**